Further observations on the dimerisation of alkynes on triruthenium clusters

Michael I. Bruce [a,*], Jonathan R. Hinchliffe [a], Paul A. Humphrey [a], Richard J. Surynt [a], Brian W. Skelton [b], Allan H. White [b]

[a] *Department of Chemistry, University of Adelaide, Adelaide, South Australia 5005, Australia*
[b] *Department of Chemistry, University of Western Australia, Nedlands, Western Australia 6907, Australia*

Received 18 June 1997

Abstract

The reaction between $Ru_3\{\mu_3\text{-PPhCH}_2PPh(C_6H_4)\}(CO)_9$ (**2**) and HC_2Ph resulted in insertion of a diene formed by coupling of the alkyne into an Ru–P(phosphido) bond to give a $PPh(C_6H_4)CH_2PPh(C_4H_2Ph_2)$ ligand. Thermolysis regenerated the original phosphido–phosphine ligand and the alkyne dimer, which was coordinated in the usual $2\eta^1:\eta^4$-mode. Similar metallacyclopentadiene

(5)

(8a)

(8b)

(9)
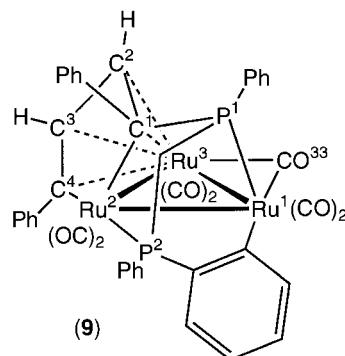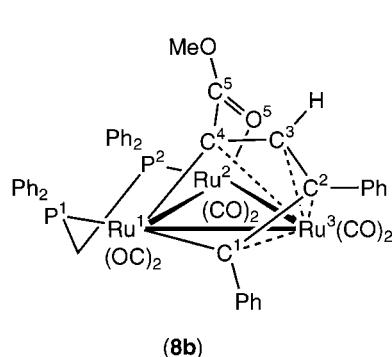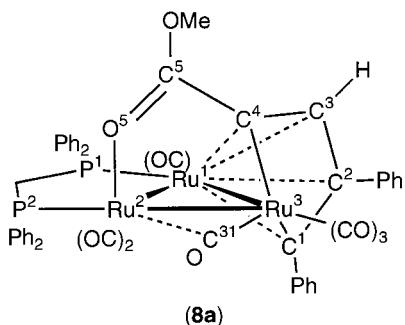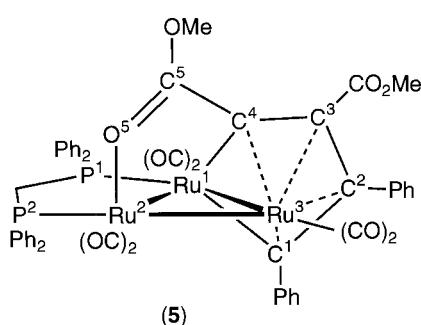
---
* Corresponding author.

complexes were obtained from **2** and HC_2CO_2Me, from $Ru_3\{\mu_3\text{-}RC_2(CO_2Me)\}(\mu\text{-dppm})(\mu\text{-CO})(CO)_7$ and C_2Ph_2 [R = CO_2Me, H (2 isomers)], and from $[Ru_3(\mu_3\text{-PPhCH}_2PPh_2)(CO)_9]^-$ and C_2Ph_2, followed by protonation. X-ray structures are reported for the complexes $Ru_3\{\mu_3\text{-}C_2Ph_2C_2(CO_2Me)_2\}(\mu\text{-dppm})(CO)_6$ (**5**) and two isomers of $Ru_3\{\mu_3\text{-}C_2Ph_2\,CHC(CO_2Me)\}(\mu\text{-dppm})(CO)_6$ (**8a** and **8b**), $Ru_3\{\mu_3\text{-PPh}(C_6H_4)CH_2PPh(C_4H_2Ph_2)\}(\mu\text{-CO})(CO)_6$ (**9**) and $Ru_3(\mu\text{-H})(\mu_3\text{-PPhCH}_2PPh_2)(\mu\text{-}C_4Ph_4)(CO)_6$ (**12**). In **5**, **8a** and **8b**, one of the ester CO groups is bonded to an Ru atom also coordinated to phosphorus.
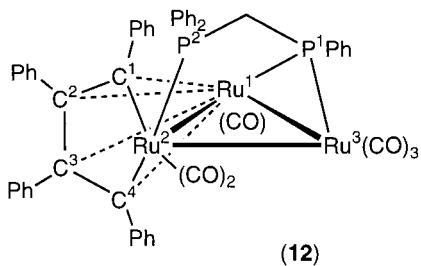
(**12**)

1. Introduction

Reactions of alkynes with $Ru_3(CO)_{12}$ have produced a variety of different complexes, containing either the cluster-bound alkyne or ligands formed by coupling of two or more alkyne molecules [1,2]. It is generally believed that formation of these complexes occurs by initial complexation of the alkyne to the cluster. Subsequent oxidative addition of 1-alkynes to the cluster may afford hydrido–alkynyl complexes. Further reactions between these complexes and additional alkyne have produced examples of complexes containing metallacyclic systems; if suitable functional groups are present, further bonding to the third metal atom may occur.

Some years ago, we described several reactions between alkynes and ruthenium cluster carbonyls substituted by tertiary phosphines, including $Ru_3(CO)_{10}(PMe_2Ph)_2$ [3], $Ru_3(\mu\text{-dppm})(CO)_{10}$ (**1**) [4,5] and $Ru_3\{\mu_3\text{-PPhCH}_2PPh(C_6H_4)\}(CO)_9$ (**2**) [4]. These reactions afforded either simple alkyne complexes, hydrido–alkynyl clusters, or compounds containing dimers of the alkyne.

The isolation of complexes containing a μ_3-alkyne naturally prompted a study of their further reactions with different alkynes described herein. These reactions were expected to afford complexes containing ligands formed by coupling of the incoming alkyne with that complexed to the cluster. In one case, the reaction of **2** with alkyne resulted in initial coupling of the alkyne with the phosphido–phosphine ligand, which was followed by P–C bond cleavage to give the metallacyclopentadiene derivative.

2. Results and discussion

We described earlier [4] the reaction between $C_2(CO_2Me)_2$ and $Ru_3(\mu\text{-dppm})(CO)_{10}$ to give the alkyne complex $Ru_3\{\mu_3\text{-}C_2(CO_2Me)_2\}(\mu\text{-dppm})(\mu\text{-}CO)(CO)_7$ (**3**) and $Ru_3\{\mu_3\text{-}C_4(CO_2Me)_4\}(\mu\text{-dppm})(CO)_6$ (**4**), in which one of the CO_2Me groups is coordinated to the ruthenium not involved in the dimetallacyclopentadiene system. We further showed that **3** reacted with more $C_2(CO_2Me)_2$ to give **4** (Scheme 1).

The reaction between **3** and C_2Ph_2, carried out in refluxing THF for 5.5 h afforded a single complex, characterised by an X-ray study (see below) as $Ru_3\{\mu_3\text{-}C_2Ph_2C_2(CO_2Me)_2\}(\mu\text{-dppm})(CO)_6$ (**5**) (Scheme 1), the analogue of **4**. The infrared spectrum contained one strong and three medium intensity $\nu(CO)$ bands at 2019, 1997, 1965 and 1954 cm^{-1}, respectively, values close to those found for **4**. In the ^1H NMR spectrum, the two nonequivalent OMe groups are found at δ 2.95 and 3.49, while the dppm CH_2 protons resonate as doublets of triplets at δ 4.73 and 5.30. The FAB mass spectrum contains M^+ at m/z 1177 and fragment ions $[M-nCO]^+$ ($n = 1$–6). These ions, like all others mentioned below, had the expected isotopic patterns.

Reactions between 1-alkynes and **1** gave hydrido–alkyne complexes $Ru_3(\mu\text{-H})(\mu_3\text{-}C_2R)(\mu\text{-dppm})(CO)_7$ in good yield [5]. We have since found that the product obtained from **1** and HC_2CO_2Me, in excellent yield, is the red μ_3-alkyne complex $Ru_3(\mu_3\text{-}HC_2CO_2Me)(\mu\text{-dppm})(\mu\text{-CO})(CO)_7$ (**6**) (Scheme 2), analogous to **3**. Complex **6** was readily identified by the presence of a $\nu(CO)$ band at 1853 cm^{-1}, consistent with the presence of a bridging CO group as required by the formulation

involving eight CO groups found in the FAB mass spectrum (M^+ at m/z 997 and peaks corresponding to the loss of nine CO groups and an OMe group). The ^{1}H NMR spectrum contains a singlet at δ 3.65 (OMe), two ABXY multiplets at δ 4.43 and 4.86 (CH$_2$ of dppm), the aromatic Ph multiplet at δ 7.37 and a triplet at δ 9.47, characteristic of the acetylenic H atom, which is coupled to both P nuclei.

The orange hydrido–alkynyl complex Ru$_3$(μ-H)(μ_3-C$_2$CO$_2$Me)(μ-dppm)(CO)$_7$ (**7**) was obtained in low yield by heating **6** in refluxing THF for 2 h. The infrared spectrum contains terminal ν(CO) absorptions and a weak band at 1861 cm^{-1}, while the FAB mass spectrum contains M^+ at m/z 969, corresponding to the loss of one CO ligand from **6**. Further fragmentation gives ions similar to those found in the spectrum of **6**, corresponding to the loss of eight CO groups and the OMe fragment. The ^{1}H NMR spectrum contains the characteristic high-field resonance at δ −19.78 as a doublet by coupling to only one of the two P nuclei of the dppm ligand and confirming the presence of the cluster-bound H atom. The OMe + CH$_2$ and Ph resonances are found as complex multiplets between δ 3.33–4.88 and 7.37, respectively, while the characteristic low-field signal for the ≡CH hydrogen atom is missing.

The reaction between **6** and diphenylethyne was carried out in refluxing THF for 2.5 h. Two isomeric complexes Ru$_3$\{μ_3-C$_2$Ph$_2$CHC(CO$_2$Me)\}(μ-dppm)(CO)$_6$ (**8a** and **8b**) were isolated from the reaction mixture, each being obtained in about 9% yield. These complexes formed black crystals and were distinguished by their infrared ν(CO) spectra. That for **8a** contained two very strong bands at 2052 and 2001 cm^{-1} and a medium intensity band at 1962 cm^{-1}, whereas that for **8b** contained a single very strong band at 1999 cm^{-1} and two medium intensity bands at 1968 and 1957 cm^{-1}; other weaker bands were present in both spectra. In the ^{1}H NMR spectra, the CH part of the alkyne-derived ligand resonated at δ 5.97 and 6.81, respectively. The FAB mass spectra were essentially identical, each containing M^+ at m/z 1119 and frag-
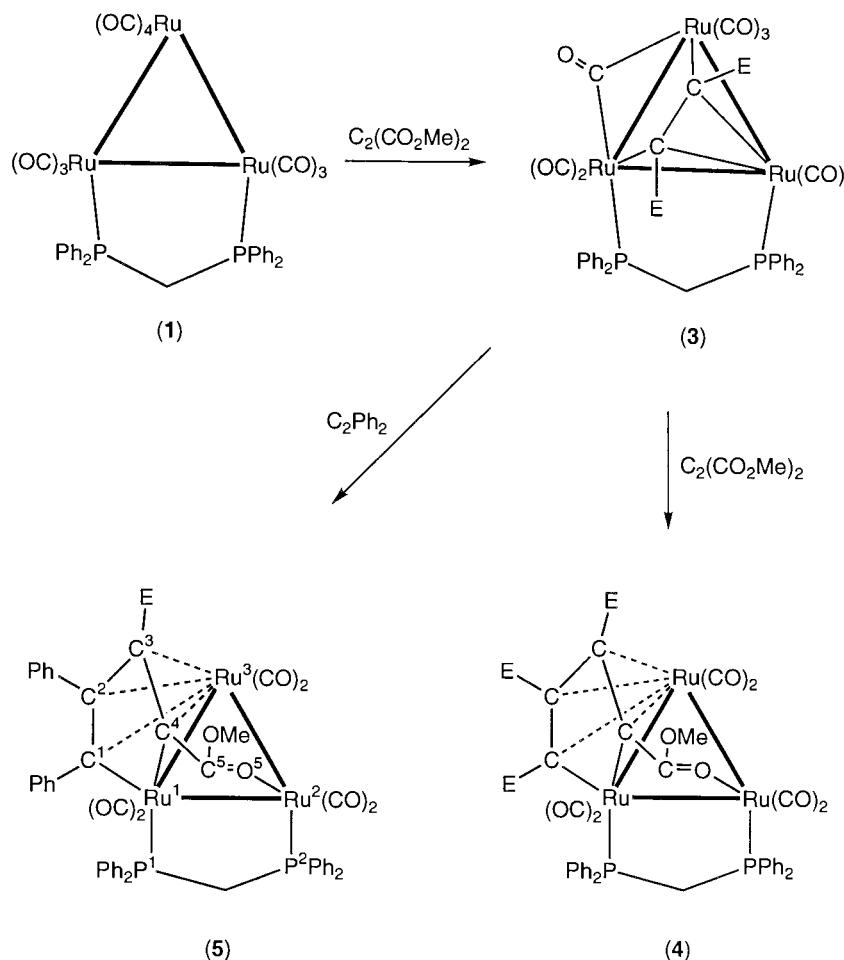
Scheme 1. E = CO$_2$Me.

ment ions formed by the stepwise loss of up to six CO groups. The structures of the two complexes were resolved by single-crystal X-ray determinations.

2.1. Molecular structures of $Ru_3\{\mu_3-C_2Ph_2C_2(CO_2Me)_2\}(\mu\text{-}dppm)(CO)_6$ (5) and two isomers of $Ru_3\{\mu_3-C_2Ph_2CHC(CO_2Me)\}(\mu\text{-}dppm)(CO)_6$ (8a) and (8b)

The similarities between these three structures are such that all three can be discussed together. Complex **8a** was obtained as a CH_2Cl_2 solvate. Molecules of **5**, **8a** and **8b** are shown in Figs. 1–3, respectively. Selected structural parameters are listed in Table 1.

All three have, as common features, a triangle of Ru atoms, one edge of which is bridged by the dppm ligand and a metallacyclopentadiene ligand formed by linking of the coordinated alkyne and free C_2Ph_2 ligand. There are no unusual features about the coordination of the dppm ligand, Ru–P distances being within the range 2.289(3)–2.376(2) Å. Internal angles at P are between 110.1(3)–116.6(1)° and at C(0), between 111.3(3) and 112.7(2)°. The Ru(1)–Ru(2) edge bridged by the dppm ligand varies between 2.697(2) and 2.8796(7) Å, the separation apparently being determined by the nature of the organic ligand attached to Ru(1) (see below). In **5**

and **8b**, the Ru(2)–Ru(3) separations are similar, at 2.683(1) and 2.6789(7) Å, respectively.

In both isomers of **8**, there is an RuCPhCPhCHCC(OMe)O cycle; the difference between **8a** and **8b** is found in its arrangement relative to the dppm ligand. In **8a**, the C_4 array is η^4 bonded to Ru(1) [also carrying P(1) of the dppm ligand] while C(1) and C(4) chelate Ru(1) to give a metallacyclopentadiene; in **5** and **8b**, the reverse situation is found. In both complexes, the other Ru atom attached to P(2) of the dppm, is coordinated by the ester CO group.

The organic ligand bridges the Ru(1)–Ru(3) vector, this separation varying from 2.701(1) to 2.744(1) Å. The Ru–C(1,4) separations [2.08(1)–2.210(4) Å] are generally shorter than those found for the inner carbons [Ru–C(2,3) 2.224(7)–2.293(8) Å] and are similar to those found for binuclear complexes of the type $Ru_2(\mu-2\eta^1:\eta^4\text{-}C_4R_4)(CO)_6$. Within the C_4Ru ring, the C–C separations are between 1.40(1)–1.456(9) Å: there is no definite picture of bond alternation around the rings. The organic ligand always contains a CO_2Me group attached to C(4), of which the ester carbonyl oxygen atom, O(5), is coordinated to Ru(2) [Ru(2)–O(5) 2.195(3)–2.217(7) Å]. This feature was found earlier in $Ru_3\{\mu_3-C_4(CO_2Me)_4\}(\mu\text{-}dppm)(CO)_6$ where the Ru–O distance is 2.187(1) Å [4].
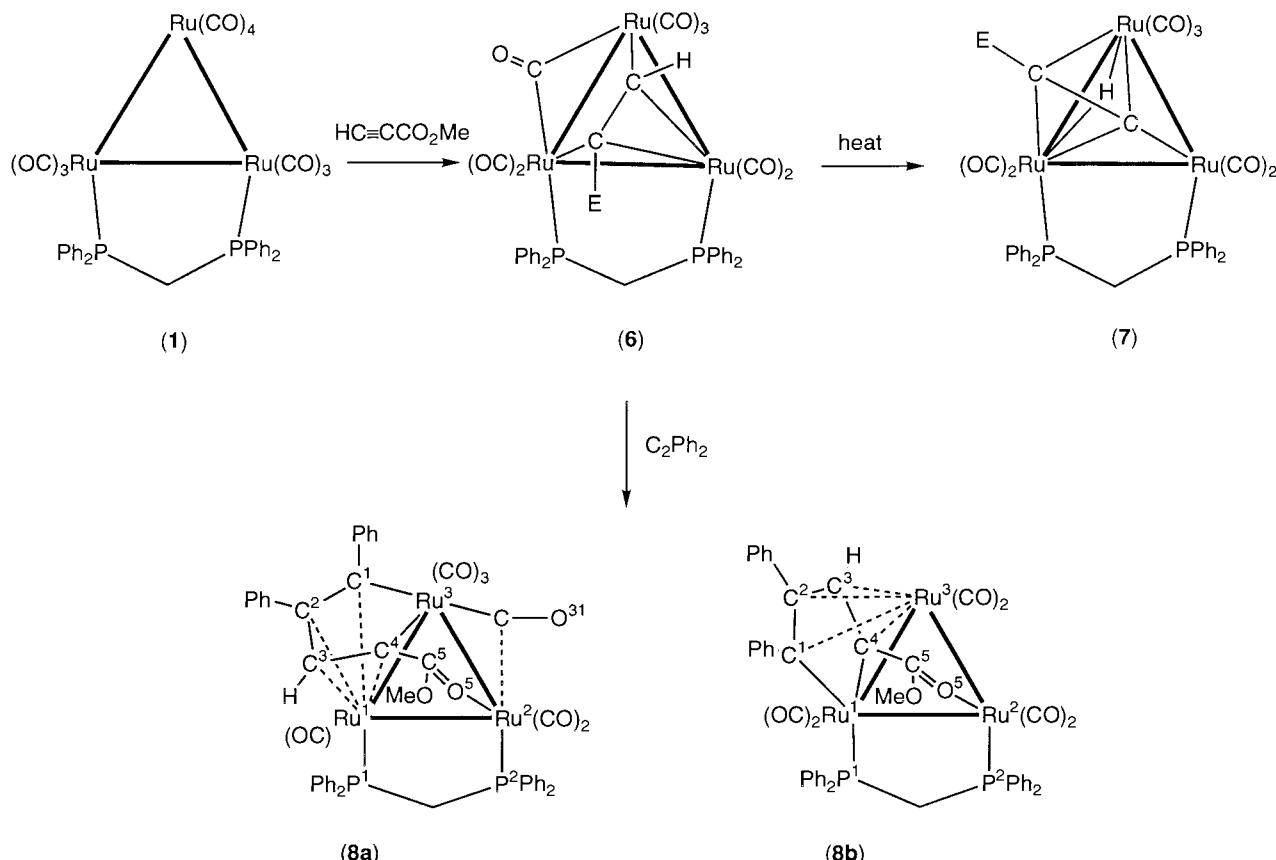
Scheme 2. E = CO_2Me.

Coordination about each Ru atom is completed by a total of six CO groups, one of which, in **8a**, semi-bridges the Ru(2)–Ru(3) vector [Ru(2)–Ru(3) 2.830(1) Å; Ru(2,3)–C(31) 2.77, 1.95(1) Å; Ru(3)–C(31)–O(31) 167.5(9)°]. Each Ru atom achieves an 18-electron count: the clusters are electron-precise with 48 cluster valence electrons.

The remarkable differences in Ru–Ru separations can be related to the orientation of the C_4 array. The shortest Ru–Ru bonds are all those that link Ru atoms coordinated to O(5) and the C_4 ligand in the η^4 mode. Conversely, the longest Ru–Ru separations are those linking Ru(2) to the Ru atom which is doubly σ bonded to the C_4 array. This is easily understood by considering the competing requirements of back-bonding to the η^4-dienyl group and the σ bonding nature of both O(5) and C(1,4), which result in a build-up of electron density of Ru(2) and the σ-bonded Ru atom.

2.2. Reactions of $Ru_3\{\mu_3\text{-}PPhCH_2PPh\}C_6H_4)\}(CO)_9$ with 1-alkynes

The most interesting products were found from the reactions between $Ru_3\{\mu_3\text{-}PPhCH_2PPh(C_6H_4)\}(CO)_9$ (**2**) and HC_2R (R = Ph or CO_2Me) (Scheme 3). The reaction with phenylethyne proceeded readily in refluxing THF after 1 h, during which time the colour changed from orange-red to dark red. Isolation of the product by preparative TLC gave a complex in 21% yield which was characterised as the heptacarbonyl complex $Ru_3\{\mu_3PPh(C_4H_2Ph_2)CH_2PPh(C_6H_4)\}(\mu\text{-}CO)(CO)_6$ (**9**) by a single-crystal X-ray study.

2.3. Molecular structure of $Ru_3\{\mu_3\text{-}PPh(C_6H_4)CH_2PPh(C_4H_2Ph_2)\}(\mu\text{-}CO)(CO)_6$ (**9**)

Fig. 4 shows a molecule of **9**, and significant bond parameters are collected in Table 2. The molecule is
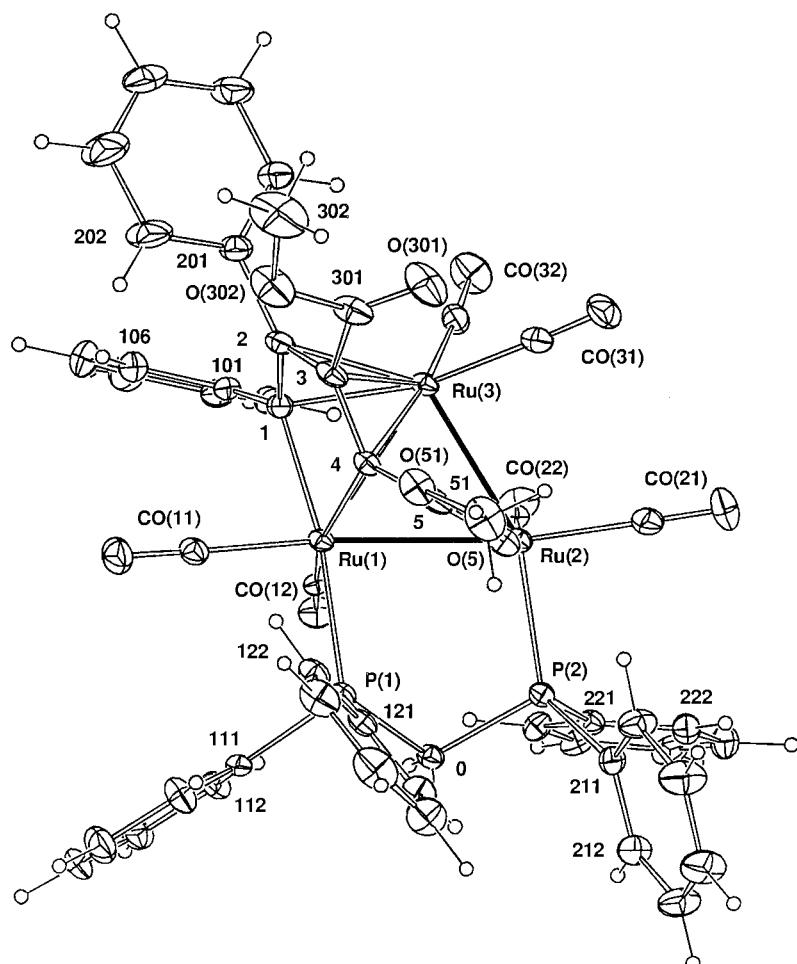
Fig. 1. Plot of a molecule of $Ru_3\{\mu_3\text{-}C_2Ph_2C_2(CO_2Me)_2\}(\mu\text{-}dppm)(CO)_6$ (**5**), showing the atom numbering scheme. In this and subsequent figures, nonhydrogen atoms are shown with 20% thermal envelopes; hydrogen atoms have arbitrary radii of 0.1 Å. Settings of the figures correspond to the scheme.

based on a triangle of Ru atoms that is spanned by the ligand formed by coupling of the two alkynes with the phosphido–phosphine originally present in **2**. Although the resulting C_4 unit chelates Ru(2) [Ru(2)–C(1,4) 2.15, 2.24(1) Å], it is attached by only three carbons to Ru(3) [Ru(3)–C(2,3,4) 2.17–2.24(1) Å] because C(1), bearing a Ph substituent, is also attached to the phosphido group [P(1)–C(1) 1.80(1) Å].

The Ru–Ru separations range between 2.769(2) and 2.911(3) Å, the former being comparable to those found in the three structures above for the Ru–Ru bond bridged by the organic ligand. Atoms P(1) and P(2) bridge the Ru(1)–Ru(2) vector by normal two-electron donor interactions [Ru(1)–P(1) 2.354(4), Ru(2)–P(2) 2.342(4) Å]. Unusually, atom P(1) occupies an axial coordination site on Ru(1), whereas P(2) is in an equatorial site on Ru(2), presumably because of the steric requirements of the other, coordinated, C_4 substituent on P(1).

Atom C(1) is four-coordinate, although angles about this carbon range between 92.9(6) [Ru(2)–C(1)–P(1)] and 122.8(7)° [Ru(2)–C(1)–C(101)]; the distortion from tetrahedral geometry is again ascribed to the steric constraints imposed by coordination to the metal triangle.

Complex **9** thus contains a ligand formed by coupling of two molecules of the alkyne and the phosphido carbon of the dephenylated metallated dppm ligand.

This ligand is attached to the Ru_3 cluster by two Ru–C σ-bonds from the ends of the C_4 chain formed by linking of the two alkyne moieties, an η^3 interaction of three atoms of this C_4 chain with the second Ru atom, and by an Ru–C σ bond and two Ru–P bonds to the $PPhCH_2PPh(C_6H_4)$ part of the ligand. Coordination is completed by two terminal CO ligands on each Ru atom and a CO group bridging one of the Ru–Ru bonds.

On heating **9** for a short time, or the original reaction mixture for a longer period, conversion to the hexacarbonyl $Ru_3\{\mu_3\text{-}PPhCH_2PPh(C_6H_4)\}(\mu\text{-}C_4H_2Ph_2)(CO)_6$ (**10**) occurs. This complex, which has been described earlier [5], contains a CPhCHCHCPh ligand bridging one of the Ru–Ru bonds, together with the metallated phosphido–phosphine ligand found in precursor **2**.

From the reaction between **2** and methyl propiolate, the only isolated product was identified as $Ru_3\{\mu_3\text{-}PPhCH_2PPh(C_6H_4)\}\{\mu\text{-}C_4H_2(CO_2Me)_2\}(\mu\text{-}CO)(CO)_6$ (**11**), the analogue of **10** with CO_2Me groups replacing the phenyl groups. We were not able to detect any intermediate analogous to **9** in this reaction. However, **11** was obtained in only 8% yield. It was characterised on the basis of similarities in its spectral properties to those of **10**. Thus, the infrared spectrum contained two very strong and two strong $\nu(CO)$ bands between 2068 and 2012 cm^{-1}, and the FAB mass spectrum contained
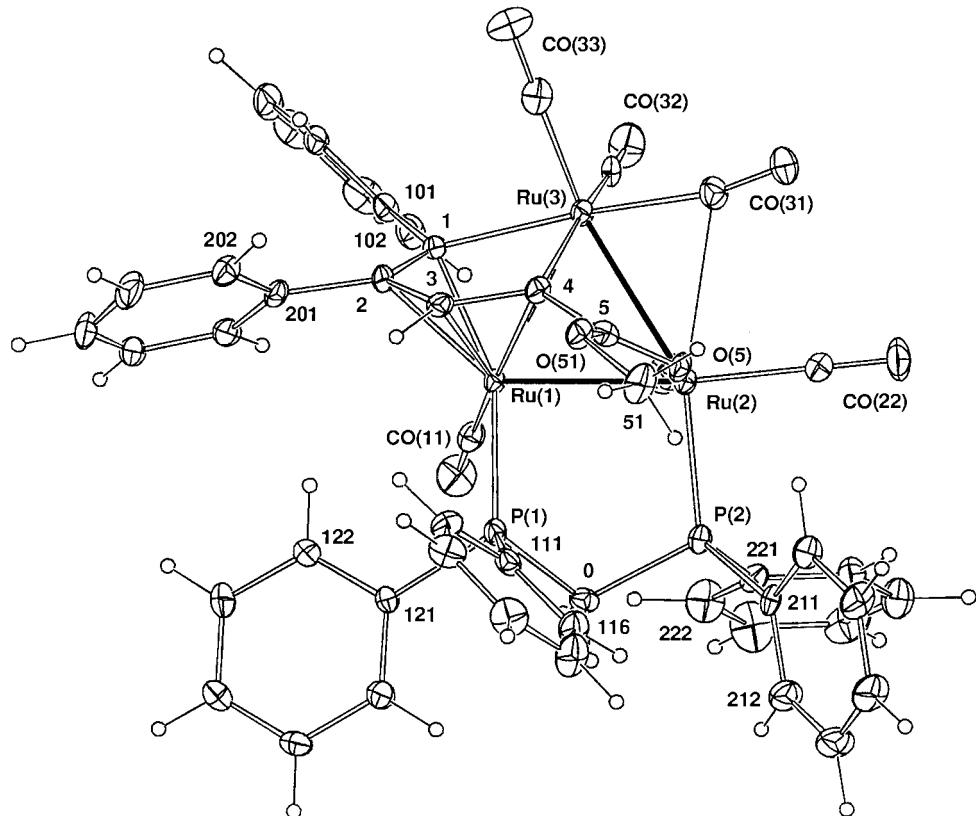

Fig. 2. Plot of a molecule of $Ru_3\{\mu_3\text{-}C_2Ph_2CHC(CO_2Me)\}(\mu\text{-}dppm)(CO)_6$ (isomer **8a**), showing the atom numbering scheme.

M^+ at m/z 975 and peaks formed by loss of up to seven CO groups. The ^1H NMR spectrum contained OMe resonances at δ 3.52 and 3.85, a C_4 ring proton at δ 2.96, the CH_2 (dppm) protons at δ 5.69 and 6.02, and complex multiplets for the second C_4 ring proton, the C_6H_4 group and the Ph groups between δ 6.82 and 8.45. The small amount obtained precluded our examining its possible further transformation to an analogue of **10**.

2.4. Related chemistry: synthesis and structure of $Ru_3(\mu\text{-}H)(\mu_3\text{-}PPhCH_2PPh_2)(\mu\text{-}C_4Ph_4)(CO)_6$ (**12**)

We were also interested to look at the reactions of anionic clusters related to the dephenylated Ru_3-dppm clusters studied above. From the reactions of the anion $[Ru_3(\mu_3\text{-}PPhCH_2PPh_2)(CO)_9]^-$ [6] and C_2Ph_2, followed by protonation (H_3PO_4), a single product could be isolated in about 55% yield. This was characterised crystallographically as the metallacyclopentadiene cluster $Ru_3(\mu\text{-}H)(\mu_3\text{-}PPhCH_2PPh_2)(\mu\text{-}C_4Ph_4)(CO)_6$ (**12**)

(Scheme 4), formed by dimerisation of C_2Ph_2 on the ruthenium cluster, a reaction which has been described on several previous occasions. The spectroscopic properties of **12** include an IR $\nu(CO)$ pattern containing five medium to strong bands, the high-field ^1H NMR resonance at $\delta - 14.38$ and an M^+ ion at m/z 1137 in the mass spectrum.

Fig. 5 is a representation of a molecule of **12**, and significant bond parameters are collected in Table 2. The triangular Ru_3 core has three different Ru–Ru separations ranging between 2.663 and 3.034(1) Å. The μ_3-PPhCH$_2$PPh$_2$ ligand is similar to other examples, with Ru–P distances of between 2.275–2.387(3) Å, and merits no further comment. The C_4Ph_4 ligand bridges the Ru(1)–Ru(2) vector, being attached to Ru(2) by two Ru–C σ-bonds [Ru(2)–C(1,4) 2.168(7), 2.11(1) Å] and to Ru(1) by all four carbons. The Ru(2)–C_4 ring interaction is tilted, the Ru(2)–C separations increasing from 2.153–2.284(8) Å.

These complexes can be related isolobally to the binuclear derivatives $Ru_2(\mu\text{-}C_4R_4)(CO)_6$ by replace-
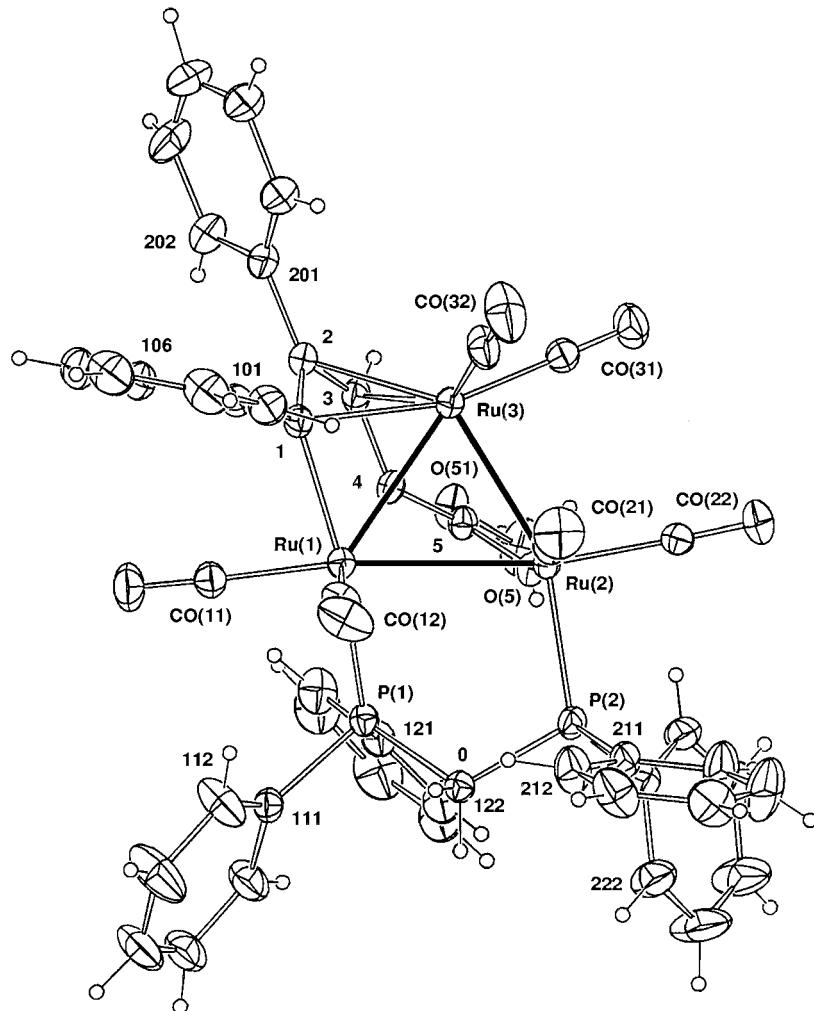
Fig. 3. Plot of a molecule of $Ru_3\{\mu_3\text{-}C_2Ph_2CHC(CO_2Me)\}(\mu\text{-}dppm)(CO)_6$ (isomer **8b**) showing the atom numbering scheme.

Table 1
Selected structural parameters for **5** and **8a**, **8b**

	5	**8a**	**8b**
Bond lengths (Å)			
Ru(1)–Ru(2)	2.860(1)	2.697(2)	2.8796(7)
Ru(1)–Ru(3)	2.744(1)	2.701(1)	2.7299(8)
Ru(2)–Ru(3)	2.683(1)	2.830(1)	2.6789(7)
Ru(1)–P(1)	2.376(2)	2.314(3)	2.368(1)
Ru(2)–P(2)	2.305(2)	2.289(3)	2.300(1)
Ru(2)–O(5)	2.214(4)	2.217(7)	2.195(2)
Ru(1)–C(1)	2.141(6)	2.174(8)[a]	2.154(5)
Ru(1)–C(4)	2.111(5)	2.08(1)[a]	2.109(4)
Ru(3)–C(1)	2.177(7)	2.144(9)[b]	2.176(5)
Ru(3)–C(2)	2.284(7)	2.293(8)[b]	2.281(5)
Ru(3)–C(3)	2.224(7)	2.27(1)[b]	2.257(4)
Ru(3)–C(4)	2.182(6)	2.201(9)[b]	2.210(4)
C(1)–C(2)	1.456(9)	1.42(1)	1.431(6)
C(2)–C(3)	1.428(8)	1.40(1)	1.434(6)
C(3)–C(4)	1.418(8)	1.40(1)	1.408(6)
C(4)–C(5)	1.471(8)	1.48(1)	1.454(6)
C(5)–O(5)	1.245(9)	1.23(1)	1.244(5)
P(1)–C(0)	1.840(7)	1.825(9)	1.838(5)
P(2)–C(0)	1.838(7)	1.842(9)	1.821(5)
Ru(3)–C(31)	1.894(7)	1.95(1)	1.867(5)
Ru(2)–C(31)	3.056(7)	2.77(1)	
Bond angles (°)			
C(1)–Ru(1)–C(4)	76.2(2)	75.2(4)[a]	75.7(2)
Ru(1)–C(1)–C(2)	114.7(4)	114.3(7)[a]	115.5(3)
C(1)–C(2)–C(3)	113.5(5)	113.9(7)	113.5(4)
C(2)–C(3)–C(4)	115.5(5)	116.0(9)	115.7(4)
C(3)–C(4)–Ru(1)	116.7(4)	117.6(7)[a]	117.1(3)
Ru(2)–O(5)–C(5)	113.3(3)	112.5(6)	112.8(2)
Ru(1)–P(1)–C(0)	114.5(2)	110.1(3)	116.6(1)
Ru(2)–P(2)–C(0)	110.5(2)	112.5(3)	110.1(2)
P(1)–C(0)–P(2)	111.3(3)	111.9(5)	112.7(2)

[a] For Ru(1), read Ru(3).
[b] For Ru(3), read Ru(1).

ment of the semi-bridging CO found for complexes having R = CO_2Me [7] or CH_2OH [8], for example, by an $Ru(CO)_4$ group, which in the case of **12** has one CO group substituted by P(2). The Ru(1)–Ru(2) separation [2.663(1) Å] is much shorter than those found for the binuclear complexes, but is comparable to the similar bonds in **8a** and **8b**. The Ru(1)–Ru(3) edge, bridged by the phosphido P(2) atom, is 2.800(1) Å and is similar to that found in $Ru_3(\mu\text{-}H)(\mu_3\text{-}PPhCH_2PPh_2)(CO)_9$ [9]. The longest edge [Ru(2)–Ru(3) 3.034(1) Å] is probably bridged by the H atom (not located in the refinement) that gives rise to the high-field resonance at δ -14.4 in the ^1H NMR spectrum. Coordination is completed by two terminal CO groups on each Ru atom to give a 48e cluster.

The major features of interest in the work reported above relate to the coupling of the alkynes and their interaction with the phosphido–phosphine, followed by the thermal cleavage of the new P–C bond to give the dienyl ligand. Coupling of two alkynes to give dienyl ligands bridging M–M bonds has been reported fre-

quently before [1], as has the fluxionality of complexes of the type $M_2(\mu\text{-}2\eta^1\text{:}\eta^4\text{-}C_4R_4)L_n$ (for example, M = Fe, L = CO, PR_3, etc.; M = Co, L = Cp) [10,11]. The mode of fluxionality is thought to involve a flipping of the C_4 ligand via a bridged intermediate, whereby the chelate σ-bonded and η^4-bonded interactions are exchanged. This has been observed previously in open-chain Fe_3 clusters and is presumably the source of the two isomers of **8** that we have obtained (Scheme 5).

Insertion of alkynes into M–PR_2 bonds has been reported earlier for several systems [12–15] and extensive studies of similar reactions of alkynes with tri-iron [16,17], and tetraruthenium phosinidene [18–20] clusters have demonstrated the ready formation and cleavage of P–C bonds. In the present work, extension of the phosphido–alkyne coupling to the Ru_3 cluster results in similar P–C bond formation and subsequent cleavage under mild conditions to regenerate the phosphido group and release the organic ligand (now a diene) to the cluster. We cannot say whether the two alkynes couple before one end inserts into the Ru–P bond, or whether a phosphino–alkyne adds the second molecule of alkyne. Of note, however, is the relatively greater reactivity of the Ru–P bond, since insertion into the Ru–C_6H_4 bond is not observed.

3. Conclusions

This work describes several further examples of the formation of metallacyclopentadiene ligands by coupling of alkynes on Ru_3 clusters also bearing dppm or ligands derived from it. In one case, two isomeric clusters were isolated, perhaps the result of the well-known oscillation of diene ligands about a metal–metal bond found in binuclear complexes. Similar reactions have been reported for the clusters $Fe_3(\mu\text{-}N_2Et_2)(\mu\text{-}CPhCHCHCPh)(CO)_7$ [21]. The reaction of C_2Ph_2 with $[Ru_3(\mu_3\text{-}PPhCH_2PPh_2)(CO)_9]^-$, followed by protonation, afforded complex **12**, which contains a C_4Ph_4 ligand formed by coupling of two C_2Ph_2 molecules on the cluster. As found in previous examples, the resulting buta-1,3-dien-1,4-diyl ligand bridges only one of the Ru–Ru bonds in the familiar $2\eta^1\text{:}\eta^4$ mode.

4. Experimental

4.1. General experimental conditions

All reactions were performed under a nitrogen atmosphere using dried, degassed solvents. No special precautions were taken to exclude air during work-up, since most complexes proved to be stable in air. Chemical reagents were commercial products and were used
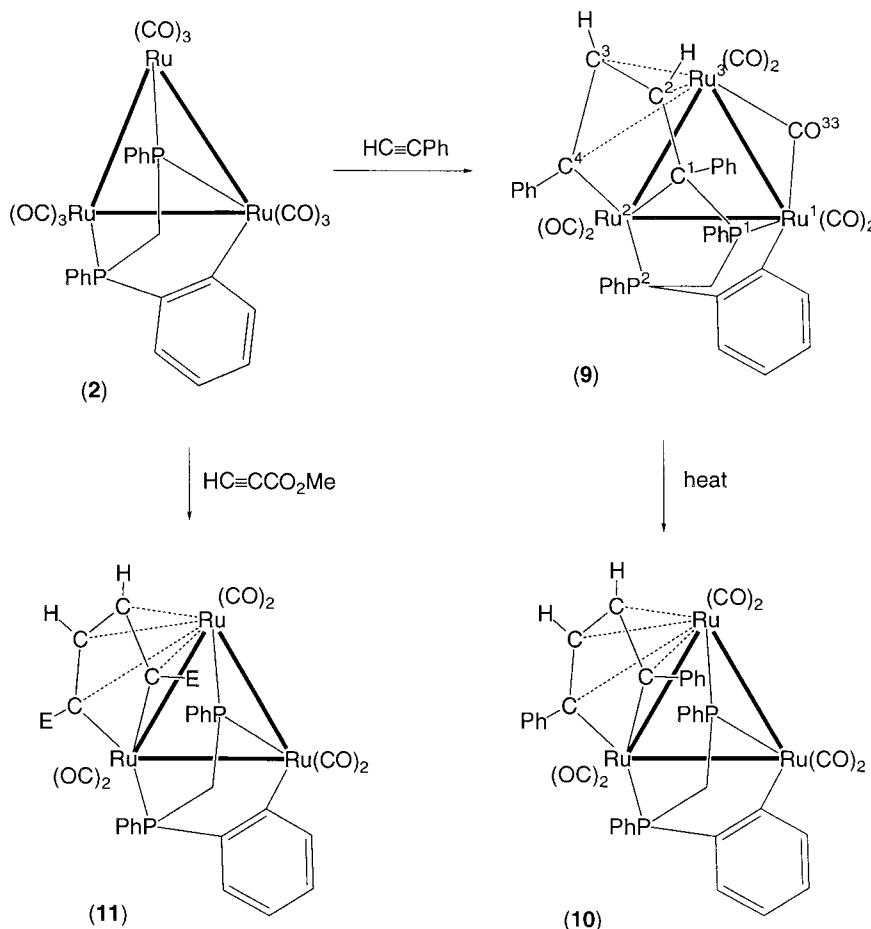
Scheme 3.

as received, unless indicated otherwise. The nitrogen used was of high purity grade and obtained from Commonwealth Industrial Gases (CIG). Solvents used for chromatography were LR grade; spectroscopic grade solvents were used for spectroscopy; all other solvents used were AR grade and/or were dried and distilled under a nitrogen atmosphere. Preparative TLC was carried out on 20×20 cm glass plates and coated with Kieselgel 60 GF_{254} silica gel (0.5 mm thick).

4.2. Instrumentation

Infrared spectra were recorded (using sodium chloride solution cells) on a Perkin Elmer 1720X FT-IR spectrometer. ^{1}H and ^{13}C NMR spectra were recorded on a Bruker ACP-300 and a Varian Gemini-200 spectrometer. FAB mass spectra were obtained on a VG ZAB 2HF instrument; ES mass spectra were measured with a VG Platform at the University of Waikato, Hamilton, New Zealand. Where specific compositions are given for ions, the observed isotopic patterns agreed with those calculated [22]; only the m/z value of the most intense peak of each cluster is reported. Elemental microanalysis were determined by the Canadian Micro-

analytical Service, Delta, British Columbia, Canada. Melting points were measured in sealed capillaries using a Gallenkamp melting point apparatus and are uncorrected.

4.3. Starting materials

The complexes $Ru_3(\mu\text{-dppm})(CO)_{10}$ [23], $Ru_3\{\mu_3\text{-}C_2(CO_2Me)_2\}(\mu\text{-dppm})(\mu\text{-CO})(CO)_7$ [4] and $Ru_3\{\mu\text{-}PPhCH_2PPh(C_6H_4)\}(CO)_9$ [9,24] were prepared by the cited literature methods.

4.4. Preparation of $Ru_3\{\mu_3\text{-}C_4(CO_2Me)_2Ph_2\}(\mu\text{-}dppm)(CO)_6$ (5)

A mixture of $Ru_3\{\mu_3\text{-}C_2(CO_2Me)_2\}(\mu\text{-dppm})(\mu\text{-}CO)(CO)_7$ (134 mg, 0.127 mmol) and C_2Ph_2 (25 mg, 0.14 mmol) was heated in refluxing THF (25 ml) for 5.5 h after which time spot TLC showed that no starting material remained. After evaporation to dryness (rotary evaporator), crystallisation from $CH_2Cl_2/MeOH$ yielded brown crystals of $Ru_3\{\mu_3\text{-}C_4(CO_2Me)_2Ph_2\}(\mu\text{-dppm})(CO)_6$ (5) (110 mg, 74%), m.p. > 200°C (dec.). Anal. Found: C, 52.08; H, 3.19%;
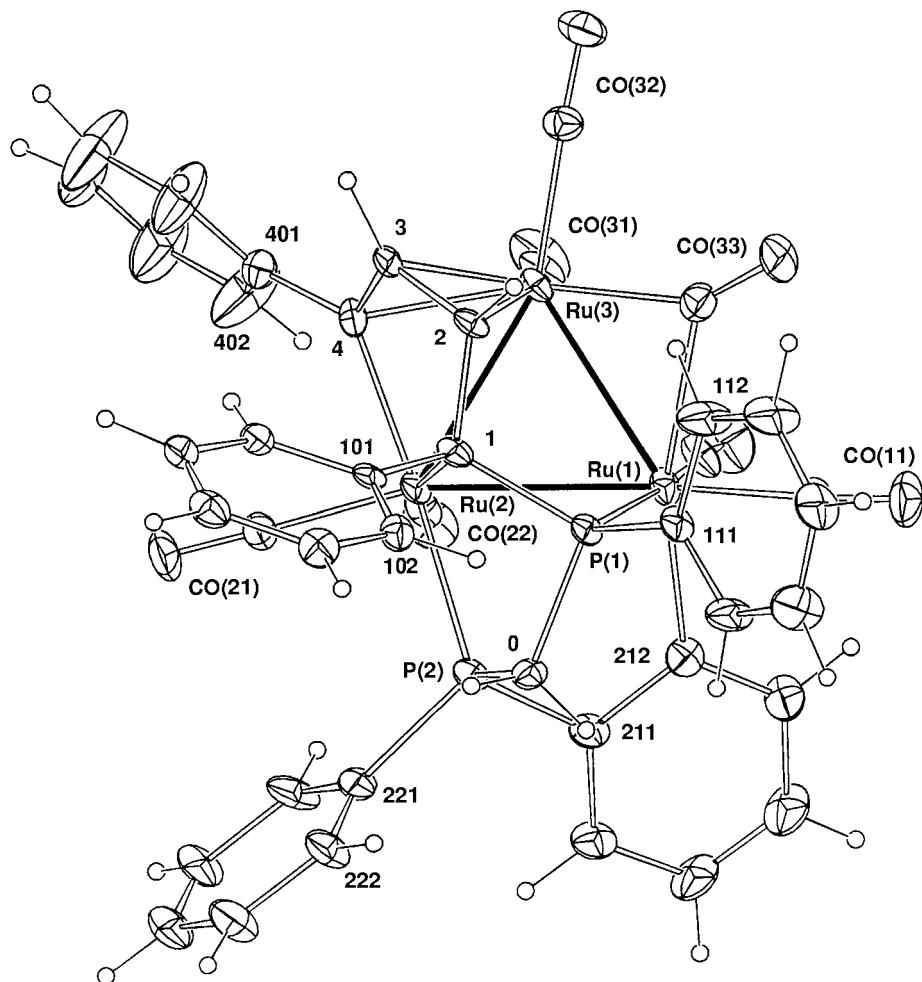
Fig. 4. Plot of a molecule of $Ru_3\{\mu_3\text{-}PPh(C_6H_4)CH_2PPh(C_4H_2Ph_2)\}(\mu\text{-}CO)(CO)_6$ (**9**), showing the atom numbering scheme.

Table 2
Selected structural parameters for **9** and **12**

Bond lengths (Å)	9	12	Bond angles (°)	9	12
Ru(1)–Ru(2)	2.911(3)	2.663(1)	C(1)–Ru(2)–C(4)	81.0(4)	76.0(4)
Ru(1)–Ru(3)	2.825(2)	2.800(1)	Ru(2)–C(1)–C(2)	98.7(7)	115.0(7)
Ru(2)–Ru(3)	2.769(2)	3.034(1)	C(1)–C(2)–C(3)	117.1(9)	115.7(7)
Ru(1)–P(1)	2.354(4)	2.275(3)	C(2)–C(3)–C(4)	114(1)	115.1(9)
Ru(2)–P(2)	2.342(4)	2.387(3)	C(3)–C(4)–Ru(2)	112.5(8)	117.8(8)
Ru(3)–P(1)	–	2.327(3)	Ru(1)–P(1)–Ru(3)		74.95(9)
Ru(1)–C(1)	–	2.153(9)	Ru(2)–P(2)–C(0)	104.7(4)	106.7(4)
Ru(2)–C(1)	2.24(1)	2.168(8)	P(1)–C(0)–P(2)	98.4(6)	109.0(6)
Ru(2)–C(4)	2.15(1)	2.11(1)	Ru(1)–P(1)–C(0)	109.4(5)	121.4(2)
Ru(3)–C(2)	2.24(1)	2.201(7)[a]	Ru(3)–P(1)–C(0)	–	115.3(3)
Ru(3)–C(3)	2.18(2)	2.269(8)[a]	C(101)–C(1)–C(2)	108(1)	115.6(7)
Ru(3)–C(4)	2.17(1)	2.284(8)[a]	Ru(2)–C(1)–P(1)	92.9(6)	
Ru(1)–C(33)	2.29(1)		P(1)–C(1)–C(2)	113.9(9)	
Ru(3)–C(33)	1.99(1)	2.01(1)	C(101)–C(1)–Ru(2)	122.8(7)	127.9(6)
P(1)–C(0)	1.84(1)	1.84(1)	Ru(1)–C(33)–O(33)	131(1)	
P(2)–C(0)	1.84(1)	1.843(9)	Ru(3)–C(33)–O(33)	147(1)	172.8(7)
C(1)–C(2)	1.54(2)	1.40(1)			
C(2)–C(3)	1.43(2)	1.44(1)			
C(3)–C(4)	1.41(1)	1.38(1)			

[a] For Ru(3), read Ru(1).
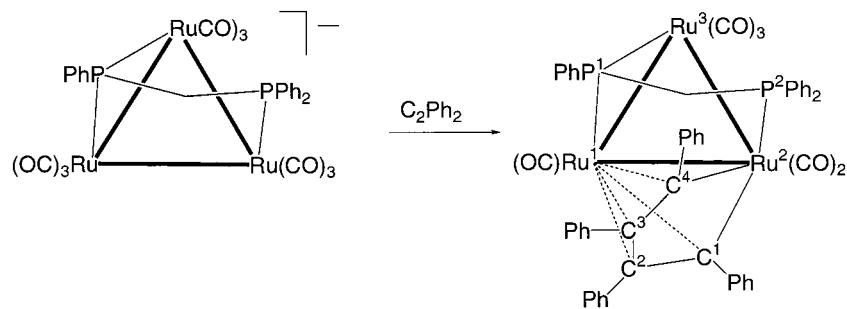
Scheme 4.

M^+, 1177. $C_{51}H_{38}O_{10}P_2Ru_3$ calcd: C, 52.00; H, 3.23%; M, 1177. Infrared (CH_2Cl_2): $\nu(CO)$ 2019m, 1997s, 1965m, 1954m, 1935w, 1912w cm^{-1}. ^1H NMR: $\delta(CDCl_3)$ 2.95 (s, 3H, OMe), 3.49 (s, 3H, OMe), 4.73 [dt, $J(HH) = 14$ Hz, $J(HP) = 11$ Hz, 1H, CH_2], 5.30 [dt, $J(HH) = 14$ Hz, $J(HP) = 11$ Hz, 1H, CH_2], 6.99–7.98 (m, 30H, Ph). FAB MS (m/z): 1177, M^+, 67; 1149, $[M–CO]^+$, 17; 1121, $[M–2CO]^+$, 33; 1093, $[M–3CO]^+$, 78; 1065, $[M–4CO]^+$, 92; 1037, $[M–5CO]^+$, 39; 1009, $[M–6CO]^+$, 100.
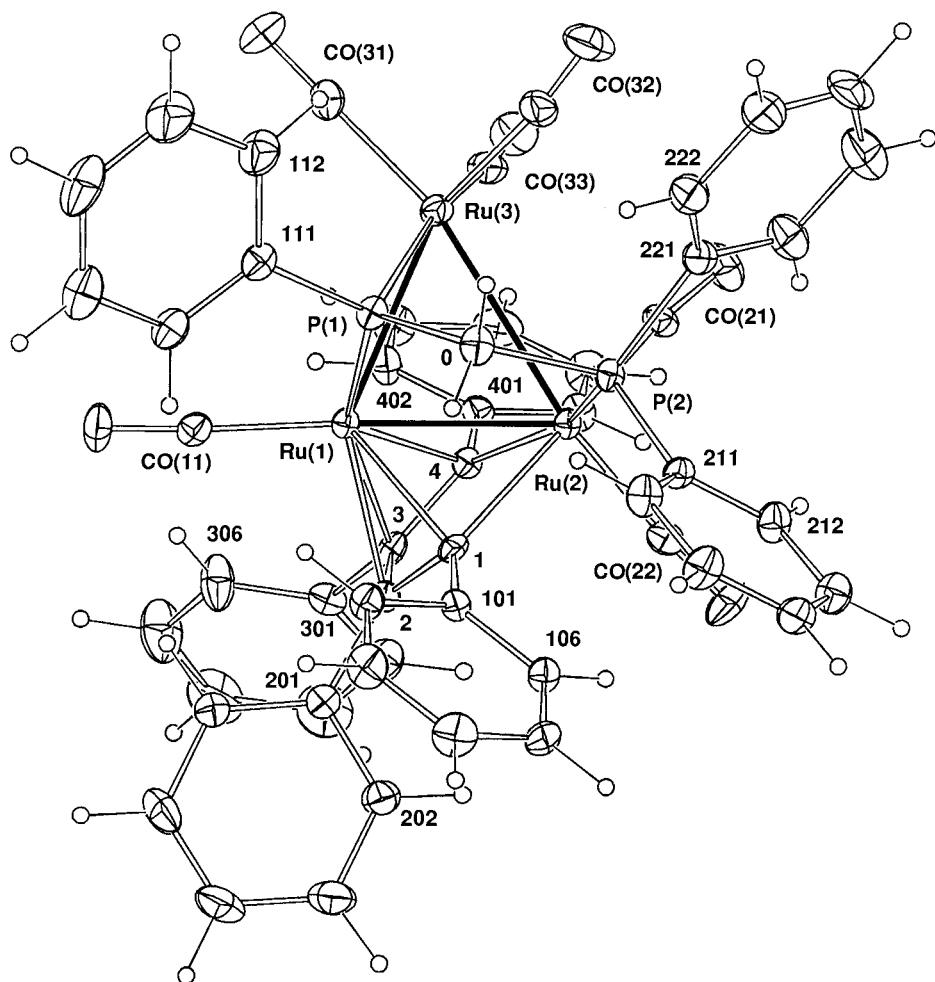
Fig. 5. Plot of a molecule of $Ru_3(\mu$-H$)(\mu_3$-PPhCH$_2$PPh$_2)(\mu$-C$_4$Ph$_4)$(CO)$_6$ (**12**), showing the atom numbering scheme.
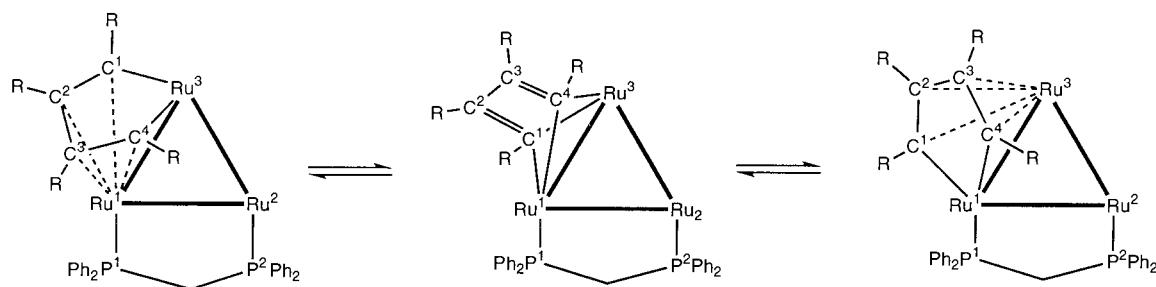
Scheme 5.

4.5. Reaction of $Ru_3(\mu\text{-}dppm)(CO)_{10}$ with HC_2CO_2Me

A mixture of $Ru_3(\mu\text{-}dppm)(CO)_{10}$ (100 mg, 0.103 mmol) and HC_2CO_2Me (13 mg, 0.155 mmol) was heated in refluxing CH_2Cl_2 (20 ml) for 3 h. After removal of solvent, the residue was separated by preparative t.l.c. (light petroleum/CH_2Cl_2 3/2) to give two bands. Band 1 (R_f 0.7) containing recovered $Ru_3(\mu\text{-}dppm)(CO)_{10}$ (10 mg, 10%). The red band (R_f 0.24) was recrystallised from CH_2Cl_2/hexane to give red crystals of $Ru_3(\mu_3\text{-}HC_2CO_2Me)(\mu\text{-}dppm)(\mu\text{-}CO)(CO)_7$ (**6**) (82 mg, 89%), m.p. > 140°C (dec.). Anal. Found: C, 42.11; H, 3.38%; M$^+$, 997. $C_{37}H_{26}O_{10}P_2Ru_3$ calcd: C, 44.63; H, 2.63; M, 997. Infrared (cyclohexane): ν(CO) 2069s, 2041m, 2023s, 2001s, 1976m, 1945m, 1853m cm^{-1}. ^{1}H NMR: δ(CDCl$_3$) 3.65 (s, 3H, OMe), 4.43 (m, ABXY pattern, 1H, CH$_2$), 4.86 (m, ABXY pattern, 1H, CH$_2$), 7.37 (m, 20H, Ph), 9.47 [t, J(HP) = 10 Hz, 1H, ≡CH]. FAB MS (m/z): 997, M$^+$; 969-745, [M–nCO]$^+$ (n = 1–9); 713, [M–9CO–OMe]$^+$.

4.6. Pyrolysis of $Ru_3(\mu_3\text{-}HC_2CO_2Me)(\mu\text{-}CO)(CO)_7$ (**6**)

A solution of $Ru_3(\mu_3\text{-}HC_2CO_2Me)(\mu\text{-}CO)(CO)_7$ (40 mg, 0.04 mmol) in THF (20 ml) was refluxed for 2 h. Purification by preparative t.l.c. (light petroleum/CH_2Cl_2 3/7) gave three bands and a brown baseline. The orange band (R_f 0.4) was recrystallised from CH_2Cl_2/MeOH to give orange crystals of $Ru_3(\mu\text{-}H)(\mu_3\text{-}C_2CO_2Me)(\mu\text{-}dppm)(CO)_7$ (**7**) (10 mg, 26%). Infrared (cyclohexane): ν(CO) 2073m, 2060s, 2043w, 2028vs, 2016s, 1999s, 1973m, 1966(sh), 1946vw, 1861w cm^{-1}. ^{1}H NMR: δ(CDCl$_3$) − 19.78 [d, J(HP) = 33 Hz, 1H, Ru–H], 3.33–4.88 (m, 5H, CH$_2$ + OMe), 7.37 (m, 20H, Ph). FAB MS (m/z): 969, M$^+$; 941-745, [M–nCO]$^+$ (n = 1–8); 713, [M–8CO–OMe]$^+$.

4.7. Reaction of $Ru_3\{\mu_3\text{-}HC_2(CO_2Me)\}(\mu\text{-}dppm)(\mu\text{-}CO)(CO)_7$ with C_2Ph_2

A mixture of $Ru_3\{\mu_3\text{-}HC_2(CO_2Me)\}(\mu\text{-}dppm)(\mu\text{-}CO)(CO)_7$ (**6**) (124 mg, 0.124 mmol) and C_2Ph_2 (25

Table 3
Crystal data and refinement details for complexes **5**, **8a**, **8b**, **9** and **12**

Compound	**5**	**8a**	**8b**	**9**	**12**
Formula	$C_{51}H_{38}O_{10}P_2Ru_3$	$C_{49}H_{36}O_8P_2Ru_3 \cdot CH_2Cl_2$	$C_{49}H_{36}O_8P_2Ru_3$	$C_{42}H_{28}O_7P_2Ru_3$	$C_{53}H_{38}O_6P_2Ru_3$
MW	1176.0	1202.9	1118.0	1009.8	1136.0
Crystal system	Triclinic	Triclinic	Monoclinic	Triclinic	Monoclinic
Space group	$P\bar{1}$	$P\bar{1}$	$P2_1/c$	$P\bar{1}$	$P2_1/c$
a (Å)	11.140(5)	17.842(8)	12.012(4)	15.453(13)	13.966(5)
b (Å)	13.053(5)	11.934(3)	16.901(4)	13.064(5)	19.214(4)
c (Å)	17.100(8)	11.698(7)	23.077(8)	10.845(8)	20.099(6)
α (°)	92.03(4)	80.01(4)		66.85(6)	
β (°)	97.34(4)	77.42(4)	98.61(3)	72.55(7)	119.48(3)
γ (°)	104.38(3)	85.39(3)		87.30(8)	
V (Å^3)	2383	2392	4632	1914	4695
Z	2	2	4	2	4
D_c (g cm^{-3})	1.64	1.67	1.60	1.75	1.61
$F(000)$	1172	1196	2224	996	2264
Crystal size (mm)	$0.35 \times 0.30 \times 0.10$	$0.16 \times 0.21 \times 0.21$	$0.47 \times 0.20 \times 0.25$	$0.20 \times 0.06 \times 0.15$	$0.26 \times 0.32 \times 0.22$
A^* (min, max)	1.11, 1.34	1.17, 1.26	1.20, 1.36	1.10, 1.45	1.21, 1.25
μ (cm^{-1})	10.4	11.7	10.9	12.7	10.7
$2\theta_{max}$ (°)	50	50	55	50	50
N	8564	8387	10608	6733	8240
N_o	5353	5389	6708	4311	5036
R	0.039	0.053	0.037	0.063	0.047
R_w	0.036	0.056	0.037	0.066	0.047

mg, 0.14 mmol) was heated in refluxing THF (22 ml) for 2.5 h, after which time the solvent was removed (in vacuo). Preparative t.l.c. (CH$_2$Cl$_2$/hexane 45/55) showed three major bands. Band 1 (colourless, R_f 0.88) was identified as C$_2$Ph$_2$ (spot t.l.c.). Band 2 (yellow-green, R_f 0.54) was crystallised from CH$_2$Cl$_2$/MeOH to give black crystals of Ru$_3${μ_3-OC(OMe)CCHC$_2$Ph$_2$}(μ-dppm)(CO)$_6$ · CH$_2$Cl$_2$ (8a) (13 mg, 8.7%). Anal. Found: C, 49.65; H, 1.94%; M$^+$ (solvent-free), 1119. C$_{49}$H$_{36}$O$_8$P$_2$Ru$_3$ calcd: C, 49.93; H, 3.18%; M, 1119. Infrared (cyclohexane): ν(CO) 2052vs, 2001vs, 1987w, 1962m, 1936w, 1891 w cm^{-1}. ^{1}H NMR: δ(CDCl$_3$) 3.22 (s, 3H, OMe), 4.66 (m, 1H, CH$_2$), 5.08 (m, 1H, CH$_2$), 5.30 (s, 2H, CH$_2$Cl$_2$), 5.97 [d, J(HP) = 4 Hz, 1H, HC], 6.39–8.16 (m, 30H, Ph). FAB MS (m/z): 1119, M$^+$; 1091-951, [M–nCO]$^+$ (n = 1–6). Band 3 (yellow-green, R_f 0.49) was crystallised (CH$_2$Cl$_2$/MeOH) to give black crystals of Ru$_3${μ_3-OC(OMe)CCHC$_2$Ph$_2$}(μ-dppm)(CO)$_6$ (8b) (13 mg, 9.4%). Anal. Found: C, 52.27; H, 3.31%; M$^+$, 1119. C$_{49}$H$_{36}$O$_8$P$_2$Ru$_3$ calcd: C, 52.64; H, 3.25%; M, 1119 Infrared (cyclohexane): ν(CO) 2020w, 1999vs,

Table 4
Nonhydrogen positional and isotropic displacement parameters (5)

Atom	x	y	z	U(eq) Å^2
Ru(1)	0.87032(5)	0.18135(4)	0.72407(3)	0.0294(2)
Ru(2)	0.81054(5)	0.37867(4)	0.75355(3)	0.0325(2)
Ru(3)	0.70143(5)	0.20489(4)	0.82251(3)	0.0330(2)
C(11)	0.9498(6)	0.0679(5)	0.7207(4)	0.043(3)
O(11)	0.9954(5)	−0.0013(4)	0.7194(3)	0.070(2)
C(12)	0.7882(5)	0.1655(5)	0.6191(4)	0.035(2)
O(12)	0.7377(4)	0.1599(3)	0.5550(2)	0.051(2)
C(21)	0.7617(7)	0.4996(5)	0.7868(4)	0.053(3)
O(21)	0.7258(6)	0.5704(4)	0.8037(3)	0.089(3)
C(22)	0.6664(6)	0.3292(5)	0.6830(4)	0.040(3)
O(22)	0.5757(4)	0.3045(4)	0.6379(3)	0.059(2)
C(31)	0.6804(6)	0.3081(5)	0.8966(4)	0.045(3)
O(31)	0.6666(5)	0.3692(4)	0.9420(3)	0.065(2)
C(32)	0.5285(6)	0.1733(5)	0.7905(4)	0.046(3)
O(32)	0.4203(4)	0.1487(4)	0.7739(3)	0.075(2)
C(1)	0.7306(5)	0.0617(5)	0.7675(3)	0.036(2)
C(101)	0.6474(6)	−0.0231(5)	0.7129(4)	0.037(2)
C(102)	0.5598(6)	0.0004(5)	0.6564(4)	0.042(3)
C(103)	0.4879(6)	−0.0746(5)	0.5990(4)	0.053(3)
C(104)	0.4999(7)	−0.1758(6)	0.5970(5)	0.068(3)
C(105)	0.5836(8)	−0.2028(5)	0.6538(5)	0.069(4)
C(106)	0.6572(7)	−0.1277(5)	0.7109(4)	0.054(3)
C(2)	0.7531(6)	0.0506(5)	0.8522(4)	0.041(3)
C(201)	0.6792(6)	−0.0426(6)	0.8905(4)	0.052(3)
C(202)	0.7318(9)	−0.1255(8)	0.9108(6)	0.114(6)
C(203)	0.661(1)	−0.2143(8)	0.9396(7)	0.134(6)
C(204)	0.5410(9)	−0.2228(7)	0.9511(6)	0.096(5)
C(205)	0.4914(7)	−0.1390(7)	0.9353(5)	0.075(4)
C(206)	0.5593(6)	−0.0508(6)	0.9033(4)	0.054(3)
C(3)	0.8421(6)	0.1395(5)	0.8945(3)	0.041(3)
C(301)	0.8606(6)	0.1500(6)	0.9841(4)	0.056(3)
O(301)	0.8395(5)	0.2164(5)	1.0238(3)	0.085(3)
O(302)	0.9044(6)	0.0687(5)	1.0109(3)	0.091(3)
C(302)	0.914(1)	0.059(1)	1.0966(5)	0.131(7)

Table 4 (continued)

Atom	x	y	z	U(eq) Å^2
C(4)	0.9020(5)	0.2183(5)	0.8474(3)	0.032(2)
C(5)	0.9800(6)	0.3223(6)	0.8813(3)	0.044(3)
O(5)	0.9685(4)	0.4053(3)	0.8510(2)	0.043(2)
O(51)	1.0624(4)	0.3224(4)	0.9444(3)	0.056(2)
C(51)	1.1342(7)	0.4236(7)	0.9801(5)	0.075(4)
P(1)	1.0448(2)	0.2939(1)	0.67704(9)	0.0315(6)
C(111)	1.1112(5)	0.2186(5)	0.6072(3)	0.033(2)
C(112)	1.0437(6)	0.1813(5)	0.5328(4)	0.041(3)
C(113)	1.0893(7)	0.1220(5)	0.4813(4)	0.051(3)
C(114)	1.2001(7)	0.0956(6)	0.5023(4)	0.059(3)
C(115)	1.2671(7)	0.1322(6)	0.5751(5)	0.067(4)
C(116)	1.2232(7)	0.1938(6)	0.6280(4)	0.055(3)
C(121)	1.1843(5)	0.3607(5)	0.7458(3)	0.037(2)
C(122)	1.2220(6)	0.3051(5)	0.8077(4)	0.046(3)
C(123)	1.3343(7)	0.3484(7)	0.8572(4)	0.065(3)
C(124)	1.4058(7)	0.4472(7)	0.8463(5)	0.080(4)
C(125)	1.3678(7)	0.5044(6)	0.7861(5)	0.071(4)
C(126)	1.2571(6)	0.4602(6)	0.7359(4)	0.055(3)
C(0)	1.0058(6)	0.3951(5)	0.6133(3)	0.036(2)
P(2)	0.9179(2)	0.4744(1)	0.66205(9)	0.0333(6)
C(211)	1.0336(6)	0.6003(5)	0.6908(4)	0.041(3)
C(212)	1.0857(6)	0.6625(5)	0.6343(4)	0.051(3)
C(213)	1.1820(7)	0.7511(6)	0.6554(4)	0.067(3)
C(214)	1.2276(8)	0.7797(6)	0.7332(5)	0.084(4)
C(215)	1.1761(8)	0.7196(6)	0.7902(4)	0.081(4)
C(216)	1.0785(7)	0.6296(6)	0.7697(4)	0.060(3)
C(221)	0.8143(5)	0.5078(5)	0.5803(3)	0.035(2)
C(222)	0.7821(7)	0.6036(5)	0.5843(4)	0.050(3)
C(223)	0.6959(7)	0.6257(5)	0.5257(4)	0.056(3)
C(224)	0.6424(6)	0.5541(6)	0.4631(4)	0.057(3)
C(225)	0.6710(6)	0.4591(5)	0.4589(4)	0.048(3)
C(226)	0.7555(6)	0.4342(5)	0.5177(4)	0.040(2)

1968m, 1957m, 1941w, 1922w cm^{-1}. ^{1}H NMR: δ(CDCl$_3$) 3.11 (s, 3H, OMe), 4.71 [dt, J(HH) = 15, J(HP) = 11 Hz, 1H, CH$_2$], 5.27 [dt, J(HH) = 15, J(HP) = 11 Hz, 1H, CH$_2$], 6.81 (s, 1H, HC), 7.05–7.94 (m, 30H, Ph). FAB MS (m/z): 1119, M$^+$; 1091-951, [M–nCO]$^+$ (n = 1–6).

4.8. Preparation of Ru$_3${μ_3-PPh(C$_4$H$_2$Ph$_2$)CH$_2$PPh-(C$_6$H$_4$))}(μ-CO)(CO)$_6$ (9)

A mixture of Ru$_3${μ_3-PPhCH$_2$PPh(C$_6$H$_4$)}(CO)$_9$ (50.3 mg, 0.058 mmol) and phenylacetylene (6.2 mg, 0.061 mmol) was heated in refluxing THF for 1 h, during which time the colour of the solution changed from orange-red to dark red. Solvent and excess phenylacetylene were removed in vacuo. The product was purified as a dark red solid by preparative t.l.c. (light petroleum/acetone 4/1) (R_f 0.40), and recrystallised (CH$_2$Cl$_2$/n-hexane) to give dark red crystals of Ru$_3${μ_3-PPh(C$_4$H$_2$Ph$_2$)CH$_2$PPh(C$_6$H$_4$)}(μ-CO)(CO)$_6$ (9) (12.1 mg, 21%). Anal. Found: C, 49.10; H, 2.82%; M$^+$, 1011. C$_{42}$H$_{28}$O$_7$P$_2$Ru$_3$ calcd: C, 49.85; H, 2.77%; M, 1011. IR: ν(CO) (cyclohexane) 2058(vs), 2040(w),

2027(s), 2014(vs), 2001(s), 1982(m), 1960(m), 1893(w) cm^{-1}. ^{1}H NMR: δ (CDCl$_3$) 2.73 [t, 1H, J(HH) = 13 Hz, CH-acetylenic], 3.67 (m, 1H, CH$_2$-dppm), 4.37 [t, 1H, J(HH) = 3 Hz, CH-acetylenic], 5.88 (m, 1H, CH$_2$-dppm), 6.41 (m, 1H, C$_6$H$_4$), 6.64–6.69 (m, 3H, acetylenic, C$_6$H$_4$ + Ph) 7.01 (m, 4H, C$_6$H$_4$ + Ph), 7.21–7.64 (m, 16H, C$_6$H$_4$ + Ph). FAB MS: (m/z): 1011, [M]$^+$; 983-815, [M–nCO]$^+$ (n = 1–7).

4.9. Pyrolysis of Ru$_3${μ_3-PPh(C$_4$H$_2$Ph$_2$)CH$_2$PPh-(C$_6$H$_4$))}(μ-CO)(CO)$_6$ (9)

A solution of Ru$_3${μ_3-PPh-(C$_4$H$_2$Ph$_2$)CH$_2$PPh(C$_6$H$_4$)}(μ-CO)(CO)$_6$ (9) (2.3 mg, 0.0023 mmol) in THF (20 ml) was heated at reflux

Table 5
Nonhydrogen positional and isotropic displacement parameters (**8a**)

Atom	x	y	z	U(eq) Å^2
Ru(1)	0.28130(5)	0.67994(7)	0.49822(6)	0.0289(3)
Ru(2)	0.19368(5)	0.60557(7)	0.71278(6)	0.0325(3)
Ru(3)	0.28355(5)	0.45267(7)	0.57270(6)	0.0327(3)
C(11)	0.2066(6)	0.7431(9)	0.4185(9)	0.041(4)
O(11)	0.1589(5)	0.7877(7)	0.3689(7)	0.069(4)
C(21)	0.1214(6)	0.5928(9)	0.6269(9)	0.045(4)
O(21)	0.0735(5)	0.5851(7)	0.5778(7)	0.068(4)
C(22)	0.1338(6)	0.5366(9)	0.8605(9)	0.046(4)
O(22)	0.0954(5)	0.4957(7)	0.9452(7)	0.074(4)
C(31)	0.2521(6)	0.3829(9)	0.7378(9)	0.047(4)
O(31)	0.2439(5)	0.3275(7)	0.8290(6)	0.068(4)
C(32)	0.2026(6)	0.3838(9)	0.5324(8)	0.044(4)
O(32)	0.1540(5)	0.3418(8)	0.5048(7)	0.074(4)
C(33)	0.3603(6)	0.344(1)	0.5288(9)	0.046(4)
O(33)	0.4082(5)	0.2762(7)	0.5032(8)	0.075(4)
P(1)	0.2781(2)	0.8586(2)	0.5511(2)	0.0324(9)
C(111)	0.3426(6)	0.8990(8)	0.6375(8)	0.038(4)
C(112)	0.4209(6)	0.8864(9)	0.5987(9)	0.046(4)
C(113)	0.4730(6)	0.9244(9)	0.654(1)	0.055(5)
C(114)	0.4468(7)	0.978(1)	0.749(1)	0.062(5)
C(115)	0.3701(8)	0.992(1)	0.791(1)	0.066(6)
C(116)	0.3173(7)	0.952(1)	0.7391(9)	0.053(5)
C(121)	0.2954(6)	0.9758(8)	0.4264(8)	0.036(4)
C(122)	0.3256(7)	0.9509(9)	0.3143(9)	0.056(5)
C(123)	0.3400(8)	1.036(1)	0.2173(9)	0.069(5)
C(124)	0.3267(7)	1.1478(9)	0.231(1)	0.056(5)
C(125)	0.2973(7)	1.1749(9)	0.341(1)	0.057(5)
C(126)	0.2819(7)	1.0880(9)	0.4388(9)	0.054(5)
C(0)	0.1813(6)	0.8964(8)	0.6275(8)	0.037(4)
P(2)	0.1415(2)	0.7814(2)	0.7467(2)	0.0341(9)
C(211)	0.1493(5)	0.8316(8)	0.8835(7)	0.035(4)
C(212)	0.1123(7)	0.9337(9)	0.9085(9)	0.056(5)
C(213)	0.1204(8)	0.974(1)	1.008(1)	0.068(6)
C(214)	0.1641(8)	0.910(1)	1.082(1)	0.070(6)
C(215)	0.2002(7)	0.811(1)	1.0609(9)	0.060(5)
C(216)	0.1924(6)	0.7690(9)	0.9602(9)	0.048(4)
C(221)	0.0386(6)	0.7951(9)	0.7540(9)	0.041(4)
C(222)	0.0049(7)	0.833(1)	0.659(1)	0.072(6)
C(223)	−0.0748(9)	0.837(1)	0.670(1)	0.089(7)
C(224)	−0.1194(7)	0.795(1)	0.777(2)	0.084(7)
C(225)	−0.0876(8)	0.754(1)	0.872(1)	0.072(6)
C(226)	−0.0101(6)	0.752(1)	0.8612(9)	0.053(5)

Table 5 (continued)

Atom	x	y	z	U(eq) Å^2
C(1)	0.3248(6)	0.5469(8)	0.3964(8)	0.036(4)
C(101)	0.3030(6)	0.5132(8)	0.2891(8)	0.036(4)
C(102)	0.2302(7)	0.5229(9)	0.2721(9)	0.050(4)
C(103)	0.2116(8)	0.493(1)	0.172(1)	0.067(6)
C(104)	0.269(1)	0.448(1)	0.092(1)	0.080(7)
C(105)	0.3438(9)	0.435(1)	0.109(1)	0.068(6)
C(106)	0.3608(7)	0.4665(8)	0.2094(8)	0.047(4)
C(2)	0.3912(5)	0.6099(8)	0.3862(7)	0.030(3)
C(201)	0.4372(5)	0.6687(8)	0.2700(8)	0.034(4)
C(202)	0.5154(6)	0.6694(9)	0.2540(9)	0.047(4)
C(203)	0.5585(7)	0.730(1)	0.151(1)	0.065(5)
C(204)	0.5215(8)	0.787(1)	0.067(1)	0.068(6)
C(205)	0.4448(8)	0.7853(9)	0.0800(9)	0.053(5)
C(206)	0.4018(6)	0.7255(8)	0.1797(8)	0.042(4)
C(3)	0.4062(5)	0.6241(8)	0.4956(8)	0.034(4)
C(4)	0.3579(5)	0.5682(8)	0.5971(7)	0.033(3)
C(5)	0.3574(6)	0.5976(8)	0.7153(8)	0.033(4)
O(5)	0.2970(4)	0.6050(6)	0.7894(5)	0.040(3)
O(51)	0.4252(4)	0.6162(6)	0.7345(5)	0.041(3)
C(51)	0.4251(7)	0.656(1)	0.8450(9)	0.058(5)
Cl(1)	−0.0217(4)	0.8679(6)	0.3286(5)	0.172(3)
Cl(2)	−0.0349(5)	0.6946(9)	0.1984(5)	0.306(7)
C(01)	0.008(1)	0.729(2)	0.297(1)	0.118(9)

point for 15 h. The orange-red product was purified by preparative t.l.c. (light petroleum/acetone 4/1) (R_f 0.44). The known complex Ru$_3${μ_3-PPhCH$_2$PPh(C$_6$H$_4$)}(μ-C$_4$H$_2$Ph$_2$)(CO)$_6$ (**10**) was identified from its IR ν(CO) spectrum (1.8 mg, 80%). IR: ν(CO) (cyclohexane) 2040(s), 2010(s), 2000(vs), 1971(w), 1959(s), 1946(w) cm^{-1} (Lit. [5]: 2041s, 2010s, 2000vs, 1970w, 1959s, 1945w cm^{-1}).

4.10. Preparation of Ru$_3${μ_3-PPhCH$_2$PPh(C$_6$H$_4$)}{μ-C$_4$H$_2$(CO$_2$Me)$_2$}(μ-CO)(CO)$_6$ (11)

The complex Ru$_3${μ_3-PPhCH$_2$PPh(C$_6$H$_4$)}(CO)$_9$ (55.9 mg, 0.067 mol) and methyl propiolate (5.4 mg, 0.66 mmol) were heated in refluxing THF for 3 h, during which time the colour of the solution changed from orange-red to red. Solvent and excess methyl propiolate were removed in vacuo. The product was purified as a dark red solid by preparative t.l.c. (light petroleum/acetone 4/1) (R_f 0.42), and recrystallised (CH$_2$Cl$_2$/n-hexane) to give red crystals of Ru$_3${μ_3-PPhCH$_2$PPh(C$_6$H$_4$)}{ μ-C$_4$H$_2$(CO$_2$Me)$_2$}(μ-CO)(CO)$_6$ (**11**) (5.1 mg, 8%). Found: C, 42.51; H, 2.89%; M$^+$, 975. C$_{34}$H$_{24}$O$_{11}$P$_2$Ru$_3$ Calc.: C, 41.84; H, 2.46%; M, 975. IR: ν(CO) (cyclohexane) 2068(vs), 2053(w), 2036(s), 2027(vs), 2012(s), 1983(m), 1978(m), 1963(w), 1923(w), 1881(w). ^{1}H NMR: δ (CDCl$_3$) 2.96 [t, 1H, J(HH) = 13 Hz, CH-acetylene], 3.52 (s, 3H, Me), 3.85 (s, 3H, Me), 5.69 (m, 1H, CH$_2$-dppm), 6.02 (m, 1H, CH$_2$-dppm), 6.82 (m, 1H, Ph + C$_6$H$_4$), 7.01 (m, 2H,

Table 6
Nonhydrogen positional and isotropic displacement parameters (**8b**)

Atom	x	y	z	U(eq) Å^2
Ru(1)	0.75617(3)	0.60352(2)	0.10595(1)	0.0442(1)
Ru(2)	0.62250(3)	0.68811(2)	0.17920(1)	0.0432(1)
Ru(3)	0.75439(3)	0.76467(2)	0.11382(2)	0.0487(1)
C(11)	0.8566(4)	0.5360(3)	0.0732(2)	0.062(2)
O(11)	0.9159(3)	0.4972(2)	0.0514(2)	0.096(2)
C(12)	0.6251(4)	0.5809(3)	0.0529(2)	0.063(2)
O(12)	0.5434(3)	0.5714(2)	0.0211(2)	0.103(2)
C(21)	0.5128(4)	0.7071(3)	0.1169(2)	0.065(2)
O(21)	0.4402(3)	0.7218(3)	0.0802(2)	0.103(2)
C(22)	0.5536(4)	0.7592(3)	0.2242(2)	0.056(2)
O(22)	0.5062(3)	0.8049(2)	0.2483(2)	0.089(2)
C(31)	0.7481(4)	0.8441(3)	0.1695(2)	0.061(2)
O(31)	0.7455(3)	0.8927(2)	0.2038(2)	0.092(2)
C(32)	0.6528(5)	0.8223(3)	0.0614(2)	0.080(2)
O(32)	0.5902(4)	0.8591(3)	0.0297(2)	0.126(2)
P(1)	0.7212(1)	0.49793(7)	0.16822(5)	0.0474(4)
C(111)	0.7256(4)	0.3975(3)	0.1380(2)	0.054(2)
C(112)	0.6822(6)	0.3825(3)	0.0816(3)	0.103(3)
C(113)	0.6712(7)	0.3060(4)	0.0603(3)	0.141(4)
C(114)	0.7017(7)	0.2438(3)	0.0946(3)	0.118(3)
C(115)	0.7474(6)	0.2573(3)	0.1508(3)	0.110(3)
C(116)	0.7600(6)	0.3332(3)	0.1727(3)	0.093(3)
C(121)	0.8184(4)	0.4863(3)	0.2361(2)	0.055(2)
C(122)	0.7861(5)	0.4652(3)	0.2891(2)	0.075(2)
C(123)	0.8694(6)	0.4505(4)	0.3373(2)	0.101(3)
C(124)	0.9782(6)	0.4557(4)	0.3325(3)	0.112(3)
C(125)	1.0122(5)	0.4781(4)	0.2815(3)	0.101(3)
C(126)	0.9322(4)	0.4935(3)	0.2332(2)	0.078(2)
C(0)	0.5778(3)	0.4906(3)	0.1865(2)	0.050(2)
P(2)	0.5278(1)	0.58358(7)	0.21302(5)	0.0498(4)
C(211)	0.3770(3)	0.5824(3)	0.1865(2)	0.060(2)
C(212)	0.3344(4)	0.5560(4)	0.1318(3)	0.087(3)
C(213)	0.2196(5)	0.5601(4)	0.1117(3)	0.101(3)
C(214)	0.1495(4)	0.5920(4)	0.1459(3)	0.106(3)
C(215)	0.1895(5)	0.6210(5)	0.1977(3)	0.132(4)
C(216)	0.3044(5)	0.6139(5)	0.2193(3)	0.111(3)
C(221)	0.5377(4)	0.5677(3)	0.2918(2)	0.064(2)
C(222)	0.4863(6)	0.5023(4)	0.3116(2)	0.101(3)
C(223)	0.4993(8)	0.4858(4)	0.3700(3)	0.147(4)
C(224)	0.5594(8)	0.5352(4)	0.4097(3)	0.143(4)
C(225)	0.6093(6)	0.6000(4)	0.3909(2)	0.105(3)
C(226)	0.5988(5)	0.6160(3)	0.3313(2)	0.070(2)
C(1)	0.8207(4)	0.6894(3)	0.0506(2)	0.052(2)
C(101)	0.7956(4)	0.6812(3)	−0.0149(2)	0.061(2)
C(102)	0.6901(5)	0.6938(3)	−0.0455(2)	0.076(2)
C(103)	0.6676(6)	0.6810(4)	−0.1052(2)	0.097(3)
C(104)	0.7533(6)	0.6548(4)	−0.1343(2)	0.110(3)
C(105)	0.8575(6)	0.6417(4)	−0.1048(2)	0.098(3)
C(106)	0.8805(5)	0.6554(3)	−0.0454(2)	0.074(2)
C(2)	0.9157(4)	0.7341(3)	0.0776(2)	0.057(2)
C(201)	0.9872(5)	0.7882(3)	0.0468(2)	0.071(2)
C(202)	1.1020(5)	0.7821(3)	0.0570(3)	0.086(3)
C(203)	1.1677(6)	0.8326(4)	0.0281(3)	0.121(4)
C(204)	1.1197(7)	0.8876(4)	−0.0092(3)	0.128(4)
C(205)	1.0067(6)	0.8949(4)	−0.0202(3)	0.107(3)
C(206)	0.9397(5)	0.8439(3)	0.0077(2)	0.087(3)
C(3)	0.9353(4)	0.7274(3)	0.1403(2)	0.055(2)
C(4)	0.8630(3)	0.6756(3)	0.1646(2)	0.047(2)
C(5)	0.8602(3)	0.6767(3)	0.2274(2)	0.048(2)
O(51)	0.9567(2)	0.6811(2)	0.2630(1)	0.066(1)
C(51)	0.9517(5)	0.6784(4)	0.3256(2)	0.098(3)
O(5)	0.7695(2)	0.6726(2)	0.2472(1)	0.049(1)

Ph + C$_6$H$_4$), 7.33–7.79 (m, 10H, Ph + C$_6$H$_4$), 8.23 [dd, 1H, J(HH) = 2, 8 Hz, Ph + C$_6$H$_4$], 8.45 [d, 1H, J(HH) = 2 Hz, Ph + C$_6$H$_4$]. FAB MS: (m/z) 975, M$^+$; 947-779, [M-nCO]$^+$ (n = 1–7).

Table 7
Nonhydrogen positional and isotropic displacement parameters, (**9**)

Atom	x	y	z	U(eq) Å^2
Ru(1)	0.26147(7)	0.2742(1)	0.5341(1)	0.0413(5)
Ru(2)	0.28483(6)	0.27182(9)	0.2588(1)	0.0347(4)
Ru(3)	0.12882(6)	0.34603(9)	0.3934(1)	0.0382(5)
C(11)	0.2377(9)	0.225(1)	0.728(1)	0.051(7)
O(11)	0.2171(7)	0.188(1)	0.850(1)	0.084(6)
C(12)	0.2910(9)	0.428(1)	0.489(1)	0.057(7)
O(12)	0.3115(8)	0.517(1)	0.468(1)	0.099(8)
C(21)	0.3250(9)	0.242(1)	0.094(1)	0.050(7)
O(21)	0.3503(7)	0.230(1)	−0.010(1)	0.096(8)
C(22)	0.3544(9)	0.410(1)	0.180(1)	0.049(7)
O(22)	0.3989(7)	0.4921(9)	0.135(1)	0.079(6)
C(31)	0.1743(9)	0.500(1)	0.310(2)	0.058(8)
O(31)	0.2000(8)	0.592(1)	0.255(1)	0.094(7)
C(32)	0.0099(9)	0.396(1)	0.428(1)	0.047(7)
O(32)	−0.0596(6)	0.4305(9)	0.450(1)	0.070(6)
C(33)	0.1092(9)	0.296(1)	0.599(1)	0.051(7)
O(33)	0.0562(7)	0.275(1)	0.711(1)	0.104(8)
P(1)	0.2362(2)	0.0942(3)	0.5448(3)	0.035(1)
C(111)	0.1796(8)	−0.020(1)	0.714(1)	0.042(6)
C(112)	0.0841(9)	−0.026(1)	0.772(1)	0.083(8)
C(113)	0.0423(9)	−0.112(1)	0.899(2)	0.079(8)
C(114)	0.088(1)	−0.186(1)	0.973(1)	0.065(7)
C(115)	0.180(1)	−0.178(1)	0.924(2)	0.087(9)
C(116)	0.2246(9)	−0.093(1)	0.796(1)	0.068(8)
C(0)	0.3457(7)	0.043(1)	0.479(1)	0.039(6)
P(2)	0.4025(2)	0.1743(3)	0.3359(3)	0.040(1)
C(211)	0.4588(8)	0.225(1)	0.425(1)	0.049(6)
C(212)	0.3999(8)	0.258(1)	0.528(1)	0.046(6)
C(213)	0.438(1)	0.290(1)	0.610(2)	0.063(8)
C(214)	0.532(1)	0.287(2)	0.590(2)	0.08(1)
C(215)	0.587(1)	0.259(2)	0.490(2)	0.08(1)
C(216)	0.5535(9)	0.229(1)	0.404(1)	0.058(7)
C(221)	0.4916(8)	0.137(1)	0.209(1)	0.048(7)
C(222)	0.5084(9)	0.029(1)	0.226(1)	0.062(8)
C(223)	0.570(1)	0.007(1)	0.119(2)	0.08(1)
C(224)	0.615(1)	0.093(2)	−0.004(2)	0.08(1)
C(225)	0.601(1)	0.202(2)	−0.022(2)	0.077(9)
C(226)	0.5393(9)	0.226(1)	0.083(2)	0.068(8)
C(1)	0.1912(7)	0.118(1)	0.402(1)	0.035(5)
C(101)	0.1827(7)	0.021(1)	0.360(1)	0.033(5)
C(102)	0.1851(8)	−0.092(1)	0.445(1)	0.043(6)
C(103)	0.1741(9)	−0.174(1)	0.404(1)	0.053(7)
C(104)	0.1590(9)	−0.153(1)	0.279(2)	0.052(7)
C(105)	0.1543(8)	−0.044(1)	0.195(1)	0.053(7)
C(106)	0.1682(8)	0.038(1)	0.233(1)	0.042(6)
C(2)	0.1002(7)	0.1716(9)	0.416(1)	0.033(5)
C(3)	0.0872(7)	0.253(1)	0.289(1)	0.042(6)
C(4)	0.1652(8)	0.324(1)	0.196(1)	0.040(6)
C(401)	0.1638(9)	0.404(1)	0.055(1)	0.048(6)
C(402)	0.221(1)	0.497(2)	−0.022(2)	0.13(1)
C(403)	0.218(2)	0.573(2)	−0.152(2)	0.14(1)
C(404)	0.160(2)	0.554(2)	−0.210(2)	0.10(1)
C(405)	0.101(2)	0.460(3)	−0.136(2)	0.17(2)
C(406)	0.105(1)	0.385(2)	−0.008(2)	0.11(1)

Table 8
Nonhydrogen positional and isotropic displacement parameters (**12**)

Atom	x	y	z	U(eq) Å^2
Ru(1)	0.61856(6)	0.30314(3)	0.26669(4)	0.0294(3)
Ru(2)	0.65091(6)	0.43031(3)	0.22888(4)	0.0301(3)
Ru(3)	0.79471(6)	0.37190(4)	0.38805(4)	0.0372(3)
C(11)	0.5951(7)	0.2133(5)	0.2871(5)	0.042(5)
O(11)	0.5828(6)	0.1578(3)	0.3044(4)	0.065(4)
C(21)	0.6988(7)	0.5099(5)	0.2940(5)	0.044(5)
O(21)	0.7212(6)	0.5612(3)	0.3269(4)	0.068(4)
C(22)	0.5631(7)	0.4846(5)	0.1421(5)	0.043(5)
O(22)	0.5116(6)	0.5189(4)	0.0917(4)	0.076(4)
C(31)	0.8647(8)	0.3154(5)	0.4760(6)	0.050(5)
O(31)	0.9072(6)	0.2828(4)	0.5300(4)	0.080(4)
C(32)	0.9314(9)	0.4204(5)	0.4215(5)	0.057(6)
O(32)	1.0143(6)	0.4451(4)	0.4475(4)	0.083(4)
C(33)	0.7392(8)	0.4399(5)	0.4370(5)	0.050(5)
O(33)	0.7190(6)	0.4767(4)	0.4705(4)	0.068(4)
P(1)	0.8000(2)	0.2915(1)	0.3034(1)	0.035(1)
C(111)	0.8742(7)	0.2097(5)	0.3389(5)	0.043(5)
C(112)	0.9799(8)	0.2091(6)	0.4006(6)	0.070(6)
C(113)	1.0338(9)	0.1444(7)	0.4254(8)	0.093(8)
C(114)	0.982(1)	0.0846(7)	0.3925(8)	0.087(9)
C(115)	0.879(1)	0.0848(5)	0.3312(7)	0.070(7)
C(116)	0.8249(8)	0.1473(5)	0.3059(5)	0.050(5)
C(0)	0.8563(7)	0.3243(4)	0.2437(5)	0.042(5)
P(2)	0.8104(2)	0.4148(1)	0.2158(1)	0.035(1)
C(211)	0.8025(7)	0.4258(5)	0.1220(5)	0.036(4)
C(212)	0.7544(8)	0.4861(5)	0.0815(5)	0.048(5)
C(213)	0.7479(8)	0.4999(5)	0.0120(6)	0.056(6)
C(214)	0.7913(8)	0.4514(6)	−0.0173(6)	0.055(5)
C(215)	0.8404(8)	0.3919(6)	0.0215(6)	0.057(6)
C(216)	0.8456(8)	0.3793(5)	0.0921(5)	0.051(5)
C(221)	0.9341(7)	0.4686(5)	0.2701(5)	0.044(5)
C(222)	1.0398(8)	0.4444(5)	0.2928(6)	0.062(6)
C(223)	1.1268(9)	0.4880(7)	0.3276(7)	0.081(7)
C(224)	1.115(1)	0.5557(8)	0.3409(7)	0.091(8)
C(225)	1.010(1)	0.5814(6)	0.3168(7)	0.088(8)
C(226)	0.9214(9)	0.5366(6)	0.2812(6)	0.066(6)
C(1)	0.5758(6)	0.3414(4)	0.1548(4)	0.032(4)
C(101)	0.6004(7)	0.3125(4)	0.0951(5)	0.032(4)
C(102)	0.6356(8)	0.2445(5)	0.0979(5)	0.045(5)
C(103)	0.6443(8)	0.2175(5)	0.0371(6)	0.057(6)
C(104)	0.6181(9)	0.2574(6)	−0.0262(6)	0.060(6)
C(105)	0.5837(8)	0.3241(5)	−0.0290(5)	0.051(5)
C(106)	0.5738(7)	0.3520(4)	0.0308(5)	0.040(4)
C(2)	0.4783(7)	0.3178(4)	0.1509(4)	0.033(4)
C(201)	0.4001(7)	0.2694(5)	0.0895(5)	0.037(4)
C(202)	0.3407(8)	0.2933(5)	0.0157(5)	0.053(5)
C(203)	0.2704(9)	0.2523(7)	−0.0445(6)	0.072(6)
C(204)	0.255(1)	0.1843(7)	−0.0315(7)	0.077(7)
C(205)	0.311(1)	0.1599(6)	0.0402(7)	0.090(8)
C(206)	0.38941(7)	0.2014(5)	0.1008(5)	0.063(5)
C(3)	0.4484(7)	0.3512(4)	0.2024(5)	0.036(4)
C(301)	0.3405(7)	0.3326(5)	0.1997(5)	0.038(4)
C(302)	0.2550(9)	0.3773(6)	0.1651(6)	0.066(6)
C(303)	0.154(1)	0.3608(8)	0.1604(8)	0.096(8)
C(304)	0.142(1)	0.3007(9)	0.1901(9)	0.099(9)
C(305)	0.229(1)	0.2572(7)	0.2274(9)	0.096(9)
C(306)	0.3280(9)	0.2732(5)	0.2320(7)	0.073(7)
C(4)	0.5195(6)	0.4030(4)	0.2477(4)	0.031(4)
C(401)	0.4911(7)	0.4398(4)	0.3023(5)	0.035(4)
C(402)	0.4793(7)	0.4035(4)	0.3580(5)	0.044(5)
C(403)	0.4449(8)	0.4366(6)	0.4039(5)	0.056(5)
C(404)	0.4260(8)	0.5079(6)	0.3957(6)	0.056(5)

Table 8 (continued)

Atom	x	y	z	U(eq) Å^2
C(405)	0.4370(8)	0.5436(5)	0.3418(6)	0.058(6)
C(406)	0.4707(7)	0.5104(5)	0.2957(5)	0.043(5)

4.11. Preparation of $Ru_3(\mu\text{-}H)(\mu_3\text{-}PPhCH_2PPh_2)(\mu\text{-}C_4Ph_4)(CO)_6$ (**12**)

To a stirred solution of $Ru_3(\mu\text{-dppm})(CO)_{10}$ (100 mg, 0.103 mmol) in THF (10 ml) was added $K[HBBu^s_3]$ (0.25 ml of a 0.5 M solution in THF, 0.125 mmol). The solution immediately became deep red. After stirring for 5 h at room temperature, the reaction was judged to be complete [the disappearance of the ν(CO) band of $Ru_3(\mu\text{-dppm})(CO)_{10}$ at 2078 cm^{-1} was monitored; the colour gradually lightened to orange]. Solid C_2Ph_2 (55 mg, 0.309 mmol) was added and the mixture was refluxed for 16 h. After cooling, H_3PO_4 (4 drops) was added and the mixture was reduced to dryness. A filtered (celite) CH_2Cl_2 extract (4×5 ml) was separated by preparative t.l.c. (hexane/acetone 3/1) to yield two bands. A yellow band (R_f 0.6) was recrystallised from CH_2Cl_2/MeOH to yield orange-yellow crystals of $Ru_3(\mu\text{-}H)(\mu_3\text{-}PPhCH_2PPh_2)(CO)_9$ (49 mg, 54%), identified by comparison with an authentic sample. A red band (R_f 0.4) was recrystallised from 1,2-dichloroethane/MeOH to afford red crystals of $Ru_3(\mu\text{-}H)(\mu_3\text{-}PPhCH_2PPh_2)(\mu\text{-}C_4Ph_4)(CO)_6$ (**12**) (27 mg, 23%), m.p. 254–257°C. Found: C, 54.44; H, 3.40%; M^+, 1137. $C_{53}H_{38}O_6P_2Ru_3$ calcd C, 55.94; H, 3.34%; M, 1137. Infrared (cyclohexane): ν(CO) 2079vs, 2027m, 1998s, 1988m, 1967vw, 1945w, 1931s cm^{-1}. ^{1}H NMR (CDCl$_3$): δ −14.38 [d, J(PH) = 24 Hz, 1H, Ru–H], 4.06 (m, 1H, CH$_2$), 4.81 (m, 1H, CH$_2$), 5.85–8.01 (m, 31H, Ph). ^{13}C NMR (CDCl$_3$): δ 29.69 (CH$_2$), 38.73 (ring C), 123.25–150.79 (m, Ph + ring C), 183.70–207.27 (CO).

5. Crystallography

Unique data sets were measured at ca. 295 K within the specified $2\theta_{max}$ limits using an Enraf-Nonius CAD4 diffractometer ($2\theta/\theta$ scan mode; monochromatic Mo–Kα radiation, λ 0.7107$_3$ Å); N independent reflections were obtained, N_o with $I > 3\sigma(I)$ being considered 'observed' and used in the full matrix least squares refinement after Gaussian absorption correction. Anisotropic thermal parameters were refined for the nonhydrogen atoms; $(x, y, z, U_{iso})_H$ were included constrained at estimated values. Conventional residuals R, R' on $|F|$ are quoted, statistical weights derivative of $\sigma^2(I) = \sigma^2(I_{diff}) + 0.0004\sigma^4(I_{diff})$ being used. Computation used the XTAL 3.0 program system [25] implemented by S.R. Hall; neutral atom complex scattering

factors were employed. Pertinent results are given in the figures and Tables 1–8; material deposited comprises thermal and hydrogen parameters, full molecular nonhydrogen geometries and structure factor amplitudes.

5.1. Abnormal features / variations in procedure

8b. $(x, y, z, U_{iso})_H$ were refined.

8a, **9**. Core hydrogen atom locations [H(3, 4)] were confirmed by their observation in difference maps.

12. Core hydrogen atoms were not observed in difference maps and are inferred from the chemistry.

Acknowledgements

References

[1] M.I. Bruce, in: G. Wilkinson, F.G.A. Stone, E.W. Abel, (Eds.), Comprehensive Organometallic Chemistry, Vol. 4, Pergamon, Oxford 1982, p. 858.

[2] A.K. Smith, in: E.W. Abel, F.G.A. Stone, G. Wilkinson, Comprehensive Organometallic Chemistry 2, Vol. 7, Elsevier, Oxford, 1995, p. 747.

[3] M.I. Bruce, P.A. Humphrey, H. Miyamae, A.H. White, J. Organomet. Chem. 417 (1991) 431.

[4] M.I. Bruce, P.A. Humphrey, H. Miyamae, B.W. Skelton, A.H. White, J. Organomet. Chem. 429 (1992) 187.

[5] M.I. Bruce, P.A. Humphrey, E. Horn, B.W. Skelton, E.R.T. Tiekink, A.H. White, J. Organomet. Chem. 429 (1992) 207.

[6] M.I. Bruce, M.L. Williams, J.M. Patrick, B.W. Skelton, A.H. White, J. Chem. Soc., Dalton Trans. (1986) 2557.

[7] M.I. Bruce, J.G. Matisons, B.W. Skelton, A.H. White, J. Organomet. Chem. 251 (1983) 249.

[8] A. Astier, J.C. Daran, Y. Jeannin, C. Rigault, J. Organomet. Chem. 241 (1983) 53.

[9] N. Lugan, J.J. Bonnet, J.A. Ibers, J. Am. Chem. Soc. 107 (1985) 4484.

[10] M. Rosenblum, W.P. Giering, B. North, D. Wells, J. Organomet. Chem. 28 (1971) C17.

[11] D.L. Thorn, R. Hoffmann, Inorg. Chem. 17 (1978) 126.

[12] K. Yasufuku, H. Yamazaki, J. Organomet. Chem. 35 (1972) 367.

[13] W.F. Smith, N.J. Taylor, A.J. Carty, J. Chem. Soc., Chem. Commun. (1976) 896.

[14] R. Zolk, H. Werner, J. Organomet. Chem. 252 (1983) C53.

[15] R. Regragui, P.H. Dixneuf, N.J. Taylor, A.J. Carty, Organometallics 3 (1982) 814.

[16] K. Knoll, G. Huttner, T. Fassler, L. Zsolnai, J. Organomet. Chem. 327 (1987) 255.

[17] K. Knoll, G. Huttner, T. Fassler, L. Zsolnai, J. Organomet. Chem. 332 (1987) 175, 309.

[18] J. Lunniss, S.A. MacLaughlin, N.J. Taylor, A.J. Carty, Organometallics 4 (1985) 2066.

[19] J.S. Field, R.J. Haines, E. Minshall, D.N. Smit, J. Organomet. Chem. 13 (1986) C69.

[20] J.F. Corrigan, S. Doherty, N.J. Taylor, A.J. Carty, Organometallics 12 (1993) 1365.

[21] M. Tasi, A.K. Powell, H. Vahrenkamp, Chem. Ber. 124 (1991) 1549.

[22] L.J. Arnold, J. Chem. Ed. 69 (1992) 811.

[23] M.I. Bruce, B.K. Nicholson, M.L. Williams, Inorg. Synth. 26 (1989) 271.

[24] M.I. Bruce, P.A. Humphrey, B.W. Skelton, A.H. White, M.L. Williams, Aust. J. Chem. 38 (1985) 1301.

[25] S.R. Hall, J.M. Stewart (Eds.), XTAL Users' Manual, Version 3.0, Univ. of Western Australia and Maryland, 1990.